



Effects of ocean warming on growth and distribution of dinoflagellates associated with ciguatera fish poisoning in the Caribbean



Steven R. Kibler^{a,*}, Patricia A. Tester^b, Kenneth E. Kunkel^c, Stephanie K. Moore^d,
R. Wayne Litaker^a

^a National Oceanic and Atmospheric Administration, National Ocean Service, National Centers for Coastal Ocean Science, Center for Coastal Fisheries and Habitat Research, 101 Pivers Island Road, Beaufort, NC 28516, USA

^b Ocean Tester, LLC, 381 Gillikin Road, Beaufort, NC 28516, USA

^c Cooperative Institute for Climate and Satellites, North Carolina State University and NOAA's National Climatic Data Center, Asheville, NC 28801, USA

^d University Corporation for Atmospheric Research, Joint Office for Science Support, Visiting Scientist at Northwest Fisheries Science Center, National Marine Fisheries Service, National Oceanic and Atmospheric Administration, 2725 Montlake Boulevard E, Seattle, WA 98112, USA

ARTICLE INFO

Article history:

Received 28 May 2015

Received in revised form 2 August 2015

Accepted 3 August 2015

Available online 9 September 2015

Keywords:

Climate change

Ciguatera

Harmful algal bloom

Benthic dinoflagellate

ABSTRACT

Projected water temperatures at six sites in the Gulf of Mexico and Caribbean Sea were used to forecast potential effects of climate change on the growth, abundance and distribution of *Gambierdiscus* and *Fukuyoa* species, dinoflagellates associated with ciguatera fish poisoning (CFP). Data from six sites in the Greater Caribbean were used to create statistically downscaled projections of water temperature using an ensemble of eleven global climate models and simulation RCP6.0 from the WCRP Coupled Model Intercomparison Project Phase 5 (CMIP5). Growth rates of five dinoflagellate species were estimated through the end of the 21st century using experimentally derived temperature vs. growth relationships for multiple strains of each species. The projected growth rates suggest the distribution and abundance of CFP-associated dinoflagellate species will shift substantially through 2099. Rising water temperatures are projected to increase the abundance and diversity of *Gambierdiscus* and *Fukuyoa* species in the Gulf of Mexico and along the U.S. southeast Atlantic coast. In the Caribbean Sea, where the highest average temperatures correlate with the highest rates of CFP, it is projected that *Gambierdiscus caribaeus*, *Gambierdiscus belizeanus* and *Fukuyoa ruetzleri* will become increasingly dominant. Conversely, the lower temperature-adapted species *Gambierdiscus carolinianus* and *Gambierdiscus* ribotype 2 are likely to become less prevalent in the Caribbean Sea and are expected to expand their ranges in the northern Gulf of Mexico and farther into the western Atlantic. The risks associated with CFP are also expected to change regionally, with higher incidence rates in the Gulf of Mexico and U.S. southeast Atlantic coast, with stable or slightly lower risks in the Caribbean Sea.

Published by Elsevier B.V. This is an open access article under the CC BY-NC-ND license (<http://creativecommons.org/licenses/by-nc-nd/4.0/>).

1. Introduction

Ciguatera fish poisoning (CFP) is a pantropical illness caused by the bioconcentration of algal toxins, known as ciguatoxins (CTXs), in marine food webs. CTXs are produced by benthic and/or substrate-associated dinoflagellates in the genus *Gambierdiscus* (and potentially, *Fukuyoa*, see below). There is a consensus that

CTXs enter marine food webs primarily via ingestion by herbivorous and surface-feeding fish and invertebrates (Bagnis et al., 1980, 1985; Chinain et al., 2010; GEOHAB, 2012). Growth, distribution and abundance of CFP-associated dinoflagellates are largely temperature driven and expected to shift in response to climate induced changes as ocean temperatures rise (Tester et al., 2010; Kibler et al., 2012). Historically, CFP has been more prevalent at low latitudes (~35° N–35° S), but recent evidence indicates some *Gambierdiscus* species also occur in subtropical-temperate locations where their abundance will likely increase as ocean temperatures rise (Litaker et al., 2009; Nascimento et al., 2010; Nishimura et al., 2013, 2014). In the Atlantic, CFP is most common in the Greater Caribbean Region (GCR), a broad area bounded by the coastlines of the Gulf of Mexico, Caribbean Sea, the tropical western Atlantic adjacent to the Bahamas, and the southeastern coast of the United

Abbreviations: CFP, ciguatera fish poisoning; CTX, ciguatoxins; GCR, Greater Caribbean Region; μ , growth rate; GCM, global climate model.

* Corresponding author. Tel.: +1 2527288737.

E-mail addresses: Steve.Kibler@noaa.gov (S.R. Kibler), ocean.tester@yahoo.com (P.A. Tester), Ken.Kunkel@noaa.gov (K.E. Kunkel), Stephanie.Moore@noaa.gov (S.K. Moore), Wayne.Litaker@noaa.gov (R.W. Litaker).

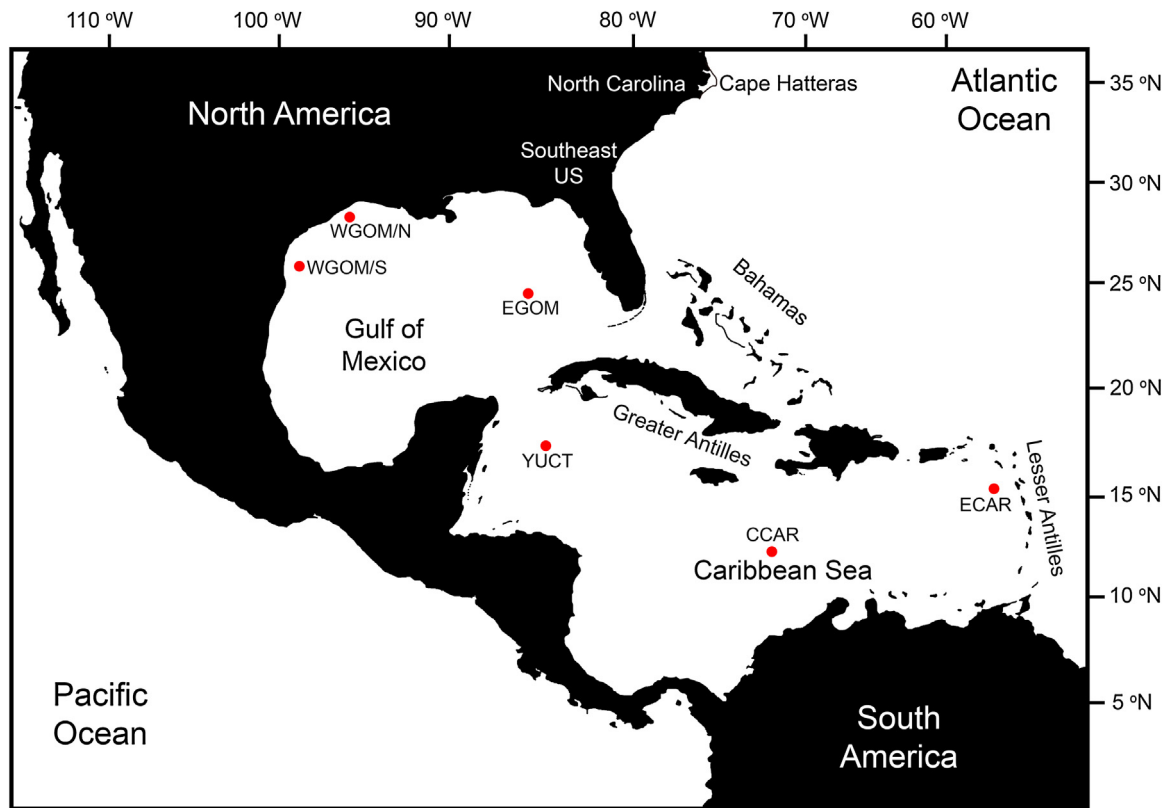


Fig. 1. Map of Caribbean region showing the six buoy sites (●) where temperature and growth were projected through the end of the 21st century. Details for each site are given in Table 1.

States as far north as Cape Hatteras, North Carolina (after Gledhill et al., 2008) (Fig. 1). Average sea surface temperatures are highest and most stable in the eastern Caribbean Sea (~24 to 29 °C), very near the optimum growth temperatures for Caribbean *Gambierdiscus* and *Fukuyoa* species (25–30 °C; Gordon, 1967; Bomber et al., 1988a; Morton et al., 1992; Gallegos, 1996; Tester et al., 2010; Kibler et al., 2012). The highest CFP incidence rates also occur in the eastern Caribbean, supporting the hypothesis that CFP occurrence is associated with optimal growth conditions for *Gambierdiscus* and *Fukuyoa* cells (Tester et al., 2010; Radke et al., 2013).

Although systematic data on cell distribution across the GCR are scarce, a review of historical records indicates *Gambierdiscus* and *Fukuyoa* cell densities tend to be greatest in warm, shallow bays and where temperatures are high and relatively stable throughout the year (Taylor and Gustavson, 1985; Bomber et al., 1989; Faust et al., 2005; Okolodkov et al., 2014; Tester et al., 2014). The case is similar in the Pacific, where CFP incidences are positively correlated with water temperatures and are highest when temperatures remain at 28–30 °C (Hales et al., 1999; Chateau-Degat et al., 2005; Llewellyn, 2010). However, the temperature–CFP relationship weakens at temperatures >30 °C, suggesting an upper thermal limit may restrict *Gambierdiscus* occurrence (Llewellyn, 2010). An upper threshold is supported by experimental data showing a precipitous decline in *Gambierdiscus* and *Fukuyoa* growth rates at temperatures approaching ~31 °C (Kibler et al., 2012). Like many tropical organisms, these dinoflagellates exhibit maximum growth rates within ~5–10 °C of their upper thermal growth limits, T_u , the point at which temperatures are too high to support cellular growth. This means that even small (1–2 °C) increases in ocean temperatures may yield relatively large increases in *Gambierdiscus*/*Fukuyoa* growth rates, but more substantial warming may cause cell mortality (Kibler et al., 2012). Such lethal temperatures are unlikely in oceanic waters, where evaporative and convective

processes prevent temperatures from exceeding ~31 °C (i.e., the ocean thermostat; Kleypas et al., 2008). However, water temperatures may approach or exceed T_u in protected coastal environments with limited vertical circulation, and coincidentally, where *Gambierdiscus* and *Fukuyoa* cells reach highest abundances (Carlson, 1984; Faust et al., 2005; Tester et al., 2014).

To better understand how rising water temperatures may affect the distribution and abundance of *Gambierdiscus* and *Fukuyoa* species in the GCR, we used experimental temperature vs. growth data in combination with projected water temperatures at six representative sites to predict how the growth rates of these species will change as oceans warm through the 21st century. Specifically, we examined the effect of rising ocean temperatures on growth of five dinoflagellate species common across the GCR (Vandersea et al., 2012): *Gambierdiscus belizeanus*, *Gambierdiscus caribaeus*, *Gambierdiscus carolinianus*, *Gambierdiscus* ribotype 2 (undescribed), and the closely related species *Fukuyoa ruetzleri* (formerly *Gambierdiscus ruetzleri*; Gómez et al., 2015). Because these species co-occur and may produce toxins causing CFP, henceforward they will be collectively referred to as CFP-associated dinoflagellates. Experimental growth data were compiled from the study by Kibler et al. (2012), together with our unpublished temperature vs. growth data from a variety of experiments completed over the last decade. Global climate model projections indicate ocean temperatures in the GCR will rise by 1–3 °C by 2100 (Good et al., 2007; Strong et al., 2008; Chollett et al., 2012). *Gambierdiscus* species are sensitive to even small increases in temperature; therefore it is likely that ocean warming will prompt changes in species abundance, diversity and distribution. It is hypothesized these changes will include (1) northward progression of species currently restricted to lower latitude environments, (2) increased abundance of species already present in subtropical to temperate areas, and (3) reduced occurrence of some species in the Caribbean Sea as temperatures exceed

their upper thermal growth limits. Because some *Gambierdiscus* species are inherently more toxic than others (Chinain et al., 1999, 2010; Lartigue et al., 2009; Litaker et al., 2010), temperature-driven shifts in species composition and abundance can affect flux of CTXs into marine food webs. It is also probable that previously unaffected areas will experience increased CFP risks (Hales et al., 1999; Chateau-Degat et al., 2005; Selig et al., 2006; Hoegh-Guldberg and Bruno, 2010; Litaker et al., 2010; Skinner et al., 2011). While this study is focused on the first order effects of temperature on *Gambierdiscus* growth, it is understood there are other environmental factors that impact *Gambierdiscus* distribution and abundance (salinity, irradiance, turbulence, substrate availability). Some of these factors and interactions will be considered in future studies.

2. Methods

2.1. Study sites and water temperature observations

Six oceanographic buoy stations were selected to represent geographically dispersed regions within the Caribbean and Gulf of Mexico based on the availability of relatively long-term water temperature data. Surface water temperatures were used to project growth rates of benthic species in the absence of sufficient data on bottom water temperatures in the GCR. While this is less than ideal, it is important to note that CFP-associated, benthic dinoflagellates are most common in shallow environments (<3 m). Water temperature data were downloaded from the website of the National Data Buoy Center (NDBC, 2015). These data were comprised of hourly surface water temperatures from oceanographic buoys located in the western Gulf of Mexico at an inshore station (WGOM/N, 29.232° N, 94.413° W) and an offshore station (WGOM/S, 29.968° N, 96.694° W), in the eastern Gulf of Mexico (EGOM, 26.044° N, 85.612° W), at a site just south of the Yucatan Strait (YUCT, 19.802° N, 84.857° W), in the central Caribbean Sea (CCAR, 14.923° N, 74.918° W) and in the eastern Caribbean Sea just west of the Lesser Antilles (ECAR, 16.332° N, 63.240° W) (Fig. 1, Table 1). The longest water temperature record was available at EGOM (1976–present), while records at stations WGOM/N and WGOM/S included data from 1993 to present and 1990 to present, respectively (Fig. 2A–C, Table 1).

Datasets from buoys at stations YUCT (2005–2013), CCAR (2005–2013) and ECAR (2009–2013) were each comprised of <10 years of data and deemed insufficient for accurate temperature projections (Table 1). To increase the length of the time series at these locations, the observed water temperature records were hindcast to 01 Jan 1990 using NOAA's Extended Reconstructed Sea Surface Temperature (ERSST) v3b gridded dataset (Smith et al., 2008; NCEI, 2015) (Fig. 3). The nearest ERSST grid point to each buoy site was selected for the hindcast water temperatures, after adjusting for the mean differences for the period when in situ and reconstructed data overlapped. The resulting reconstructed time series for the three Caribbean Sea stations are shown in Fig. 2D–F. Data from 2014 had not yet undergone the complete quality control procedures used by the NDBC, so were not included in this study.

2.2. Water temperature projections

Future scenarios for water temperature at the six stations in the Caribbean region were generated using a series of climate model simulations coordinated by the World Climate Research Programme's Working Group on Coupled Modeling (WCRP, 2015), an organization sponsored by the World Meteorological Organization (WMO), the International Council for Science (ICSU) and the Intergovernmental Oceanographic Commission (IOC) of UNESCO. Although we projected changes in ocean temperature using data

from sites only in Caribbean Sea and Gulf of Mexico, connectivity among the GCR subregions via ocean currents makes the forecasted changes in ocean temperature applicable across the entire GCR. In all, simulations from eleven global climate models (GCMs) from the WCRP consortium were selected to project water temperatures at each station in the Greater Caribbean (Fig. 3; Table 2) (Flato et al., 2013).

These GCM simulations were performed as part of the WCRP Coupled Model Intercomparison Project Phase 5 (CMIP5), which provided a standard experimental protocol for studying GCMs. The CMIP5 simulations use a set of scenarios called Representative Concentration Pathways (RCPs), based on radiative forcing trajectories. Simulations for the RCP6.0 scenario were utilized in this study. Water temperature projections were constructed by comparing the projected water temperatures with the buoy observations, and then adjusting the projected data by the difference (bias) between the observed data and the model output. The observed temperature data from each buoy [$T_{\text{obs}}(y,m)$], monthly mean values [$T_{\text{obs,mean}}(m)$] and monthly standard deviations [$\pm\sigma_{\text{obs}}(m)$] were computed by averaging the data for the period of record ($Y_{\text{beg}} - Y_{\text{end}}$), where m = month and y = year, Y_{beg} = beginning year of data and Y_{end} = ending year of data. Then monthly anomalies [$T'_{\text{obs}}(y,m)$] were computed by subtracting the monthly means:

$$T'_{\text{obs}}(y, m) = T_{\text{obs}}(y, m) - T_{\text{obs,mean}}(m) \quad (1)$$

For each model, we identified the nearest grid point to each buoy and used those data in subsequent calculations. We then applied similar calculations to the model data [$T_{\text{model}}(y,m)$] monthly mean values [$T_{\text{model,mean}}(m)$] and monthly standard deviations [$\pm\sigma_{\text{model}}(m)$] for the same period of record as the observed buoy data. Monthly anomaly values [$T'_{\text{model}}(y,m)$] were then calculated by subtracting the monthly mean value:

$$T'_{\text{model}}(y, m) = T_{\text{model}}(y, m) - T_{\text{model,mean}}(m) \quad (2)$$

The modeled temperatures were computed in the following way. For each month, a trend [$A_{\text{model}}(m)$] was computed for the model's $Y_{\text{beg}} - 2099$ time series. The model values were de-trended by subtracting the trend line values for each month:

$$T'_{\text{model,detrend}}(y, m) = T'_{\text{model}}(y, m) - A_{\text{model}}(m) \times (y - Y_{\text{beg}}) \quad (3)$$

Each detrended value [$T'_{\text{model,detrend}}(y,m)$] was then adjusted for biases in the variability of the model data, as compared to the observed data. This bias adjustment was the ratio of the standard deviations for the model and observed data. The future value of temperature for month (m) and year (y) incorporated the detrended anomaly that was adjusted for the variability bias plus the trend. The forecasted monthly temperature [$T_{\text{est}}(y,m)$] was then computed by:

$$T_{\text{est}}(y, m) = T_{\text{obs,mean}}(m) + T'_{\text{model,detrend}}(y, m) \times \pm\sigma_{\text{obs}}(m) / \times \pm\sigma_{\text{model}}(m) + A_{\text{model}}(m) \times (y - Y_{\text{beg}}) \quad (4)$$

The above downscaling approach assumes the future trend in temperature is linear, and thus a simple linear trend adjustment (A) is appropriate. An examination of the model projections (not shown) indicates that future temperature changes are indeed highly linear. This is a consequence of the choice of scenario, RCP6.0, which is characterized by an approximate linear increase in greenhouse gas forcing over the 21st century and assumes that greenhouse gas emissions will stabilize after 2080 (IPCC, 2013). Choice of another scenario with non-linear changes in greenhouse gas forcing, such as RCP4.5, would necessitate the use of a non-linear fit to the temperature change. Justification for the use of RCP6.0 follows below.

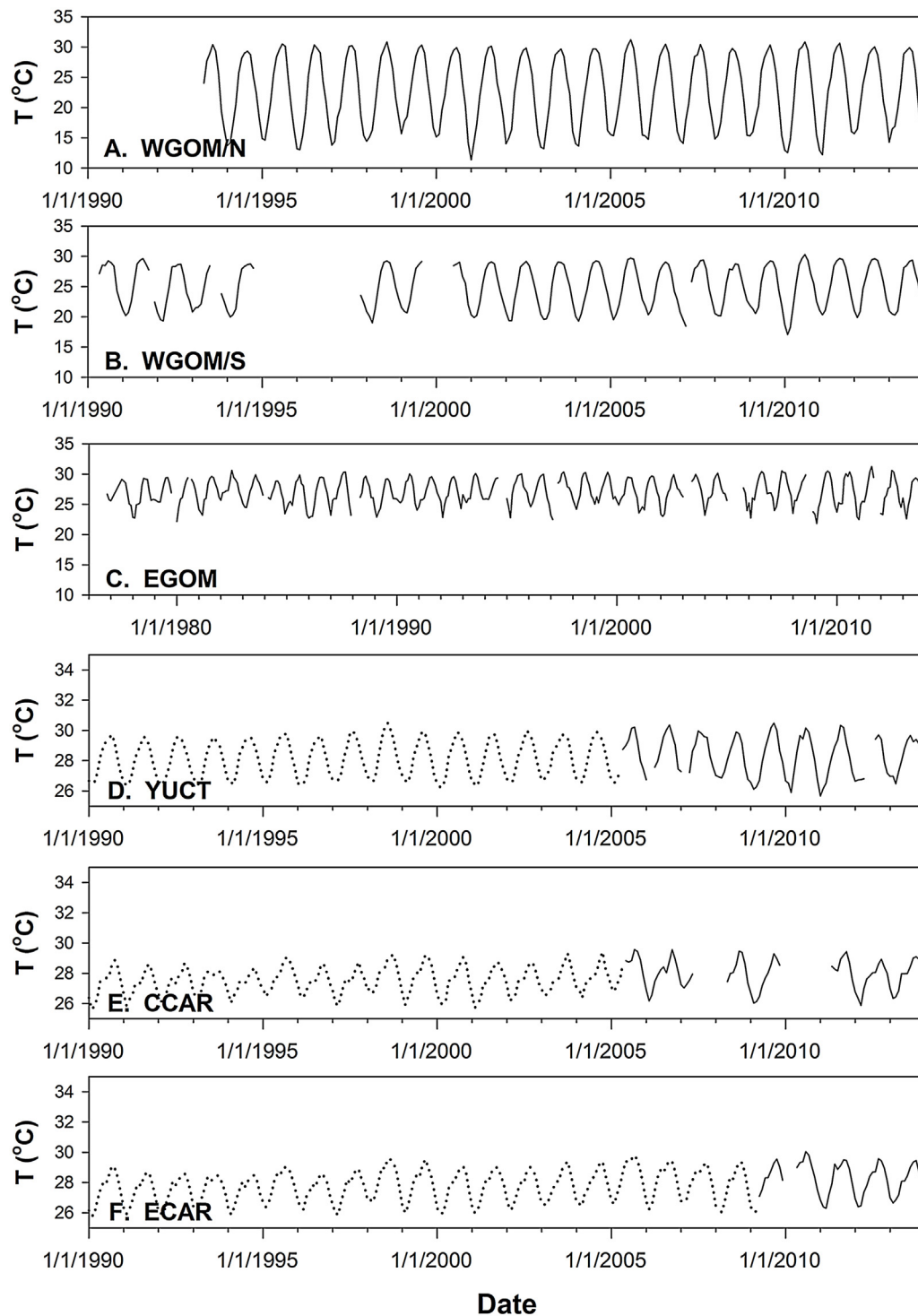


Fig. 2. In situ temperature data from buoys moored at six stations in the Gulf of Mexico and Caribbean Sea. Solid lines represent in situ data while dotted lines denote ERSST reconstructed temperatures. See text for details about each location and data reconstruction. Note longer time scale in plot C and smaller temperature scale in plots D–F.

Table 1

List of stations where in situ data were used to project surface water temperatures to 2099 using the 11 models given in Table 2. Data were downloaded from the National Data Buoy Center (NDBC).

Station	NDBC number	Latitude °N	Longitude °W	Depth (m)	Location	Span
WGOM/N	42035	29.232	94.413	14	Western Gulf of Mexico off Galveston, Texas	1993–2013
WGOM/S	42020	26.968	96.694	80	Western Gulf of Mexico off Corpus Christi, Texas	1990–2013
EGOM	42003	26.044	85.612	3274	Eastern Gulf of Mexico	1976–2013
YUCT	42056	19.802	84.857	4684	Yucatan Basin	2005–2013
CCAR	42058	14.923	74.918	4161	Central Caribbean Sea	2005–2013
ECAR	42060	16.332	63.240	1570	East Caribbean Sea west of the Lesser Antilles	2009–2013

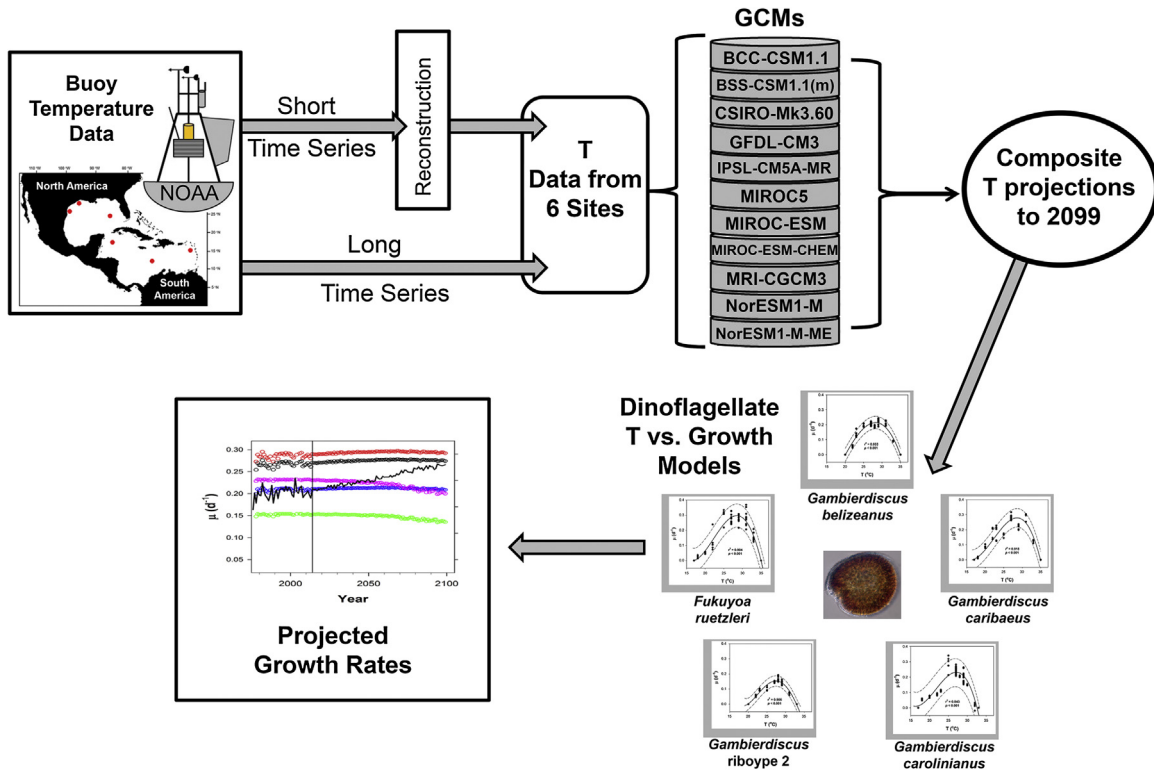


Fig. 3. Conceptual diagram detailing growth rate projections for five Caribbean *Gambierdiscus* and *Fukuyoa* species through 2099. Water temperature data (T) from three buoy sites with long time series (21–38 y) were combined with reconstructed data from three sites with short time series (5–9 y). An ensemble of 11 climate models (GCMs) were used to project water temperatures at all six buoy sites through 2099. The composite projected temperatures from each site were then combined with experimental temperature vs. growth models to projected growth rates for each dinoflagellate species. See text for details.

2.3. *Gambierdiscus* growth models

Detailed temperature vs. growth relationships were based on experimental data from Kibler et al. (2012) for five CFP-associated dinoflagellate species endemic to the Atlantic Ocean: *G. belizeanus*, *G. caribaeus*, *G. carolinianus*, *Gambierdiscus* ribotype 2 (undescribed species; see Litaker et al., 2010), and *F. ruetzleri* (previously *G. ruetzleri*). The temperature vs. growth relationships in the 2012 study were based on only one strain of each species from a single set of culture experiments. To make the growth models more representative of each species, the temperature–growth ($T - \mu$) data from Kibler et al. (2012) were supplemented with data from multiple

strains established from samples collected at sites across the GCR: *G. belizeanus* ($n = 2$), *G. caribaeus* ($n = 6$), *G. carolinianus* ($n = 5$), *Gambierdiscus* ribotype 2 ($n = 7$) and *F. ruetzleri* ($n = 2$) (Table 3). Data were compiled from experiments conducted between 2005 and 2014, with salinity (33), irradiance ($50\text{--}100 \mu\text{mol photon m}^{-2} \text{s}^{-2}$) and culture media the same as the 2012 study. This range of light levels were within the optimum growth range of each of the five species included within this study (see Kibler et al., 2012, Table 5). Growth rates for each dinoflagellate strain were determined using a larger number of data points than those in Kibler et al. (2012), yielding a more conservative measure of growth for each replicate (i.e., average rate instead of maximum rate). Experimental growth data

Table 2
Climate models used to project water temperature at each of the six stations in this study. Each model scenario was based on a global climate model (GCM) simulation from the Coupled Model Intercomparison Project Phase 5 (CMIP5), a component of the World Climate Research Programme (WCRP) Working Group on Coupled Modeling (WGCM). For details see Flato et al. (2013).

Model	No.	Climate modeling group/institution(s)	Country
BCC-CSM1.1	1	Beijing Climate Center, China Meteorological Administration	China
BCC-CSM1.1(m)	2	Beijing Climate Center, China Meteorological Administration	China
CSIRO-Mk3.6.0	3	Commonwealth Scientific and Industrial Research Organisation in collaboration with the Queensland Climate Change Centre of Excellence	Australia
GFDL-CM3	4	NOAA Geophysical Fluid Dynamics Laboratory	USA
IPSL-CM5A-MR	5	Institut Pierre-Simon Laplace	France
MIROC5	6	Atmosphere and Ocean Research Institute, The University of Tokyo/National Institute for Environmental Studies/Japan Agency for Marine-Earth Science and Technology	Japan
MIROC-ESM	7	Japan Agency for Marine-Earth Science and Technology/Atmosphere and Ocean Research Institute, The University of Tokyo/National Institute for Environmental Studies	Japan
MIROC-ESM-CHEM	8	Japan Agency for Marine-Earth Science and Technology/Atmosphere and Ocean Research Institute, The University of Tokyo/National Institute for Environmental Studies	Japan
MRI-CGCM3	9	Meteorological Research Institute, Japan Meteorological Agency	Japan
NorESM1-M	10	Norwegian Climate Centre	Norway
NorESM1-ME	11	Norwegian Climate Centre	Norway

Table 3

Strains of the five Caribbean dinoflagellate species used to generate growth vs. temperature models shown in Table 5. Abbreviation FGBNMS, Flower Garden Banks National Marine Sanctuary.

Species	Strains	Origin
<i>Gambierdiscus belizeanus</i>	CCMP399	St. Barthelemy, Caribbean
<i>G. caribaeus</i>	ST1 Gam F4	St. Thomas, U.S. Virgin Islands
	Gam19	Carrie Bow Cay, Belize
	BB4Gam1	Bathtub Beach Park, Stuart, Florida, USA
	CCMP1651	Grand Cayman, Cayman Islands, Caribbean
	Gam4	Southwater Cay, Belize
	ElbowCayAlgae Gam1	Elbow Cay, Belize
	BRPGam4 7/15/09	Southwater Cay, Belize
<i>G. carolinianus</i>	BigFish Gam5	Blowing Rock Park, Jupiter, Florida, USA
	KenNew2	North Carolina, USA
	Kenny6	North Carolina, USA
	RROV5	North Carolina, USA
	SE27-21 Gam7	Puerto Rico, USA
<i>Gambierdiscus ribotype 2</i>	CCMP1655	North Carolina, USA
	WL18Gam5	Martinique, Caribbean
	WL18Gam6	FGBNMS, NW Gulf of Mexico
	StMaartens Gam6	FGBNMS, NW Gulf of Mexico
	StMaartens Gam10	Sint Maarten, Caribbean
	EL20 T Gam3	Sint Maarten, Caribbean
	MixedPR Gam3	Dry Tortugas National Park, SE Gulf of Mexico
<i>Fukuyoa ruetzleri</i>	Gam1	Puerto Rico, USA
	NC ruetz	Southwater Cay, Belize
		North Carolina, USA

were then fit to third or fourth order polynomial equations using the curve fitting toolbox in MATLAB (R2014a, The Mathworks, Inc., Natick, MA, USA) (Fig. 4, Table 4). Inclusion of replicate growth measurements from multiple strains increased variability somewhat, but yielded more robust fit equations because of the much larger sample size ($p < 0.001$, $n = 66$ to 95, $1 - \beta > 0.999$; Zar, 1996). The results of these re-analyzed growth relationships are given in Fig. 4 and Table 4, where μ_{\max} represents the maximum fitted growth rate, T_{\max} denotes the corresponding maximum growth temperature, T_{opt} represents the range of temperatures where growth was at least 80% of μ_{\max} , and T_u and T_0 denote the upper and lower thermal limits of growth, respectively. These growth parameters (μ_{\max} , T_{\max} , T_{opt} , T_0 , T_u) were estimated using the output of each polynomial equation. The revised growth relationships yielded results

similar to those reported in Kibler et al. (2012), but with slightly lower growth rates for *G. caribaeus* (μ_{\max} 0.28 vs. 0.34 d⁻¹), *G. carolinianus* (μ_{\max} 0.23 vs. 0.29 d⁻¹) and *F. ruetzleri* (μ_{\max} 0.30 vs. 0.34 d⁻¹) (Table 4). Furthermore, T_{\max} decreased to 28.6 °C in *G. caribaeus* (from 31.4 °C) and T_u increased in *G. belizeanus*, *G. caribaeus* and *F. ruetzleri* to ~35 °C from 32 to 33 °C in the earlier study (Table 4).

Seasonal variation in CFP-associated dinoflagellate growth was evaluated using projected monthly composite temperatures at each station. Composite temperatures were ranked by month and the average for each station was calculated during four different time intervals: “2010” (2005–2014), “2030” (2025–2034), “2050” (2045–2054) and “2095” (2090–2099). Average monthly water temperatures were then used to evaluate the growth potential for

Table 4

Polynomial growth vs. temperature models for five Caribbean dinoflagellate species. Relationships were adapted using data from Kibler et al. (2012).

Species	Polynomial	μ_{\max}	T_{\max}	T_{opt}	T_0	T_u
<i>Gambierdiscus belizeanus</i>	3rd order	0.21	28.2	24.5–31.7	20.0	35.0
	Coefficients	$p_1 = -0.00010$ $p_2 = 0.00478$ $p_3 = -0.02002$ $p_4 = -0.67793$				
<i>G. caribaeus</i>	3rd order	0.28	28.6	24.5–31.9	16.5	35.0
	Coefficients	$p_1 = -0.00028$ $p_2 = 0.01840$ $p_3 = -0.37625$ $p_4 = 2.43679$				
		0.23				
	Coefficients	$p_1 = -0.00033$ $p_2 = 0.02134$ $p_3 = -0.42182$ $p_4 = 2.65837$				
<i>Gambierdiscus ribotype 2</i>	4th order	0.15	27.4	24.5–30.1	19.8	33.0
	Coefficients	$p_1 = 1.816 \times 10^{-5}$ $p_2 = -0.00214$ $p_3 = 0.08906^1$ $p_4 = -1.56085$ $p_5 = 9.78999$				
		0.30				
	Coefficients	$p_1 = 3.916 \times 10^{-6}$ $p_2 = -0.00069$ $p_3 = 0.03458$ $p_4 = -0.64459$ $p_5 = -4.04444$				
<i>Fukuyoa ruetzleri</i>	4th order	0.30	28.5	24.5–31.9	16.8	35.1
Coefficients	$p_1 = 3.916 \times 10^{-6}$ $p_2 = -0.00069$ $p_3 = 0.03458$ $p_4 = -0.64459$ $p_5 = -4.04444$					
Coefficients						

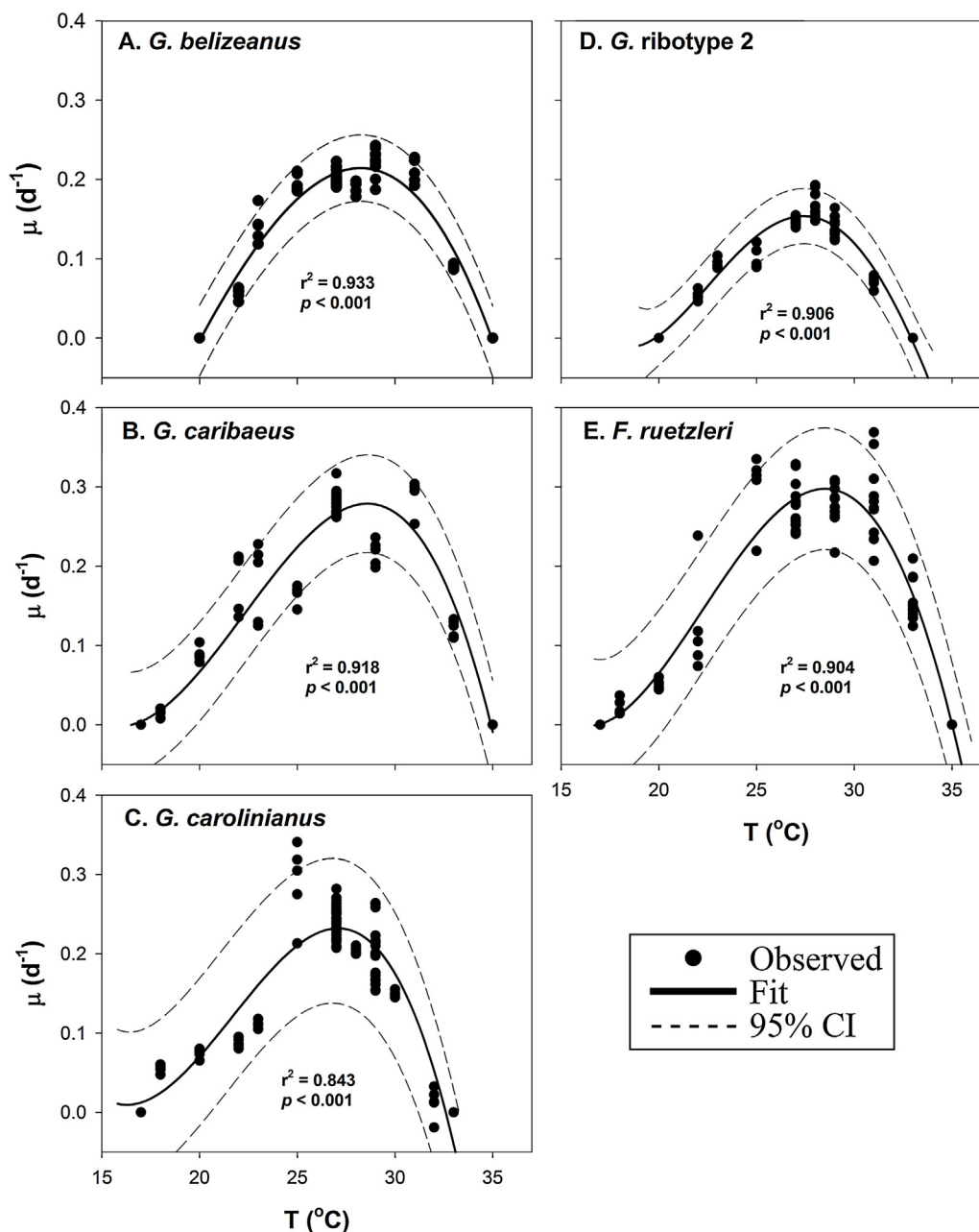


Fig. 4. Growth rate (μ , d^{-1}) vs. temperature (T , $^{\circ}\text{C}$) relationships for five Caribbean species of CFP-associated dinoflagellates: (A) *Gambierdiscus belizeanus*, (B) *G. caribaeus*, (C) *G. carolinianus*, (D) *Gambierdiscus ribotype 2*, and (E) *Fukuyoa ruetzleri*. The solid circles are measured growth rates of replicate experimental cultures from multiple strains of each species (Table 3), the solid lines represent polynomial curves fitted to the data (Table 4) and the broken lines denote upper and lower 95% confidence intervals (CI). The regression coefficient (r^2) and p -values are shown. Fit coefficients and growth model results are given in Table 4.

each of the five dinoflagellate species during each time period. The growth models were then combined with composite projected water temperatures at the six stations in the Caribbean to estimate average daily, monthly, and yearly growth rates for each of the dinoflagellate species. Daily projected temperatures were also used to calculate the number of days per year when temperature was $\leq T_0$, the number within the optimum growth range, and the number when temperature was $\geq T_u$ for each species.

3. Results

3.1. Study sites

The primary differences among observed water temperatures at the six sites were in the mean annual temperatures

as well as the magnitudes of the seasonal temperature cycles. The three Caribbean Sea locations were characterized by average temperatures (through 2013) of 28.19 ± 1.27 $^{\circ}\text{C}$, 27.69 ± 0.96 $^{\circ}\text{C}$ and 27.84 ± 1.07 $^{\circ}\text{C}$ for buoys at YUCT, CCAR and ECAR, respectively. The average temperature at buoy EGOM was slightly lower (27.04 ± 2.12 $^{\circ}\text{C}$), while temperatures at the western Gulf sites were substantially lower— 24.95 ± 3.54 $^{\circ}\text{C}$ (WGOM/S) and 22.95 ± 6.00 $^{\circ}\text{C}$ (WGOM/N) (Fig. 5).

The magnitude of vernal warming and winter cooling across the region was primarily determined by latitude, with some variation due to proximity to land and differences in ocean circulation between the eastern and western Gulf of Mexico. Buoy WGOM/N is only 30 km from shore. As a result, this site exhibited the greatest range in winter-summer temperatures (>15 $^{\circ}\text{C}$) compared with buoys WGOM/S (~ 10 $^{\circ}\text{C}$) and EGOM (~ 6 $^{\circ}\text{C}$, Fig. 2A–C).

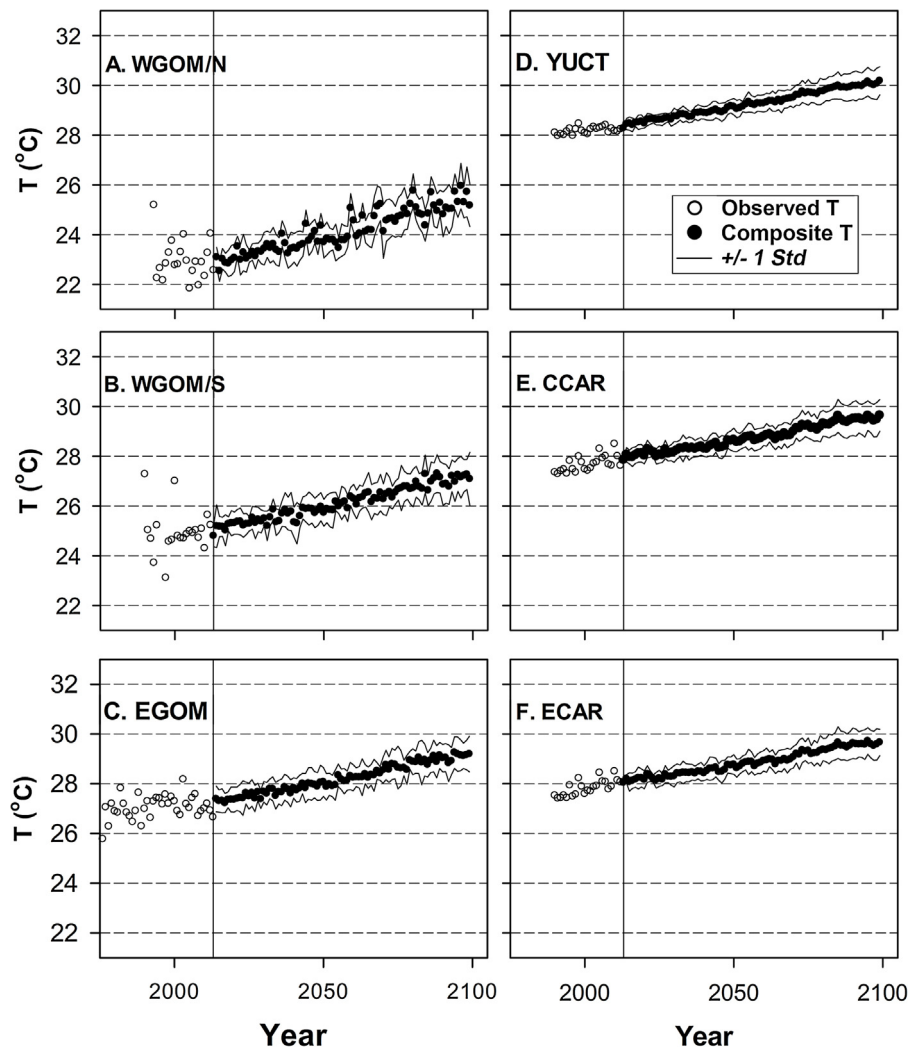


Fig. 5. Mean projected annual surface water temperature ± 1 standard deviation (std) at six stations in the Greater Caribbean region (Fig. 1). Open circles denote observed temperatures; solid circles represent projected temperatures and vertical reference lines denote the year 2013.

In comparison, the Caribbean Sea buoys (YUCT, CCAR, ECAR) exhibited relatively small seasonal temperature variations ($\leq 3.5^\circ\text{C}$), consistent with their lower latitudes ($15\text{--}20^\circ\text{N}$, Table 1, Figs. 1 and 2D–F). Winter temperatures in the western Gulf were substantially lower than observed at other sites, reaching February temperatures of $12\text{--}16^\circ\text{C}$ and $17\text{--}21^\circ\text{C}$ at WGOM/N and WGOM/S, respectively through 2013 (Fig. 2A and B). In contrast, winter temperatures never fell below 23°C at EGOM and 25°C at the three Caribbean sites (Fig. 2C–F).

3.2. Projected temperatures

All eleven model simulations projected water temperatures to increase at similar rates, although with some variability. For example, mean annual water temperature at WGOM/N is projected by the 11 models to be $22.23\text{--}24.53^\circ\text{C}$ by 2030, with a mean and standard deviation of $23.44 \pm 0.66^\circ\text{C}$ (Fig. 5A). By 2050 and 2099, temperatures at this site are projected to be $23.69 \pm 0.63^\circ\text{C}$ and $25.17 \pm 0.86^\circ\text{C}$, respectively (Fig. 5A). At station WGOM/S mean water temperatures are expected to rise from $24.79 \pm 0.43^\circ\text{C}$ in 2013 to $27.08 \pm 1.07^\circ\text{C}$ by 2099 (Fig. 5B). Slightly lower temperatures are projected in the eastern Gulf of Mexico (EGOM), where mean annual temperatures will increase from 26.65 ± 0.09 in 2013 to $29.19 \pm 0.72^\circ\text{C}$ by 2099 (Fig. 5C). The warmest conditions are projected to occur at buoy YUCT by the end of the century, where

temperatures are expected to rise from $28.28 \pm 0.00^\circ\text{C}$ during 2013 to $30.18 \pm 0.57^\circ\text{C}$ in 2099 (Fig. 5D). Comparatively, the more stable conditions in the central (CCAR) and eastern Caribbean Sea (ECAR) are expected to yield temperature increases from 27.85 and 28.04°C in 2013 to 29.64 and 29.66°C in 2099 (Fig. 5E and F). Over the entire forecast period, the average rate of temperature rise at WGOM/N was $0.27^\circ\text{C decade}^{-1}$, the most rapid rate of warming among the six stations. In comparison, the mean projected rise in temperatures at the other Gulf of Mexico sites were almost identical: $0.23^\circ\text{C decade}^{-1}$ and $0.20^\circ\text{C decade}^{-1}$ at WGOM/S and EGOM, respectively through 2099. The warming rates among the three remaining sites were almost identical: $0.20^\circ\text{C decade}^{-1}$ (YUCT), $0.20^\circ\text{C decade}^{-1}$ (CCAR) and $0.19^\circ\text{C decade}^{-1}$ (ECAR). Overall, the regional warming rate among the six sites during the forecast period averaged $0.22 \pm 0.03^\circ\text{C decade}^{-1}$.

Variability among models increased gradually through the forecast period as the climate models diverged. For example, the projected average annual temperature at WGOM/S in 2030 was $25.50 \pm 0.30^\circ\text{C}$ ($\text{CV}_{2030} = 1.2\%$), but increased to $27.08 \pm 1.07^\circ\text{C}$ ($\text{CV}_{2099} = 4.0\%$) by the end of the century (Fig. 5B). Variability among projected average annual temperatures in 2099 was similar at WGOM/N ($\text{CV}_{2099} = 3.4\%$), lower at EGOM ($\text{CV}_{2099} = 2.5\%$) and lowest at YUCT, CCAR and ECAR ($\text{CV}_{2099} = 1.8\text{--}2.2\%$). The divergence among the model projections is evidenced by the increasing size of the error bars in Fig. 5. Although CVs were generally low,

Table 5
Comparison of model results. Percentage of months when the average projected temperature predicted by each model was (A) the highest and (B) the lowest among the 11 model scenarios. Model numbers are given in Table 2.

A		Model No.										
Station	1	2	3	4	5	6	7	8	9	10	11	
WGOM/N	5	5	4	19	8	5	13	25	7	7	3	
WGOM/S	5	4	16	27	11	7	7	7	9	7	5	
EGOM	11	6	8	30	9	5	15	16	6	7	5	
YUCT	6	5	7	43	5	5	16	25	4	4	4	
CCAR	6	8	10	40	7	7	21	25	5	6	6	
ECAR	8	9	10	40	9	8	21	25	7	7	6	

B		Model No.										
Station	1	2	3	4	5	6	7	8	9	10	11	
WGOM/N	9	12	14	4	7	11	6	3	8	7	19	
WGOM/S	15	12	6	3	5	7	11	3	10	12	17	
EGOM	13	13	10	5	9	9	5	5	16	14	19	
YUCT	12	22	7	5	5	7	4	5	19	18	25	
CCAR	15	16	10	6	10	8	5	6	22	21	28	
ECAR	17	19	11	7	9	12	5	7	21	20	23	

some models consistently projected higher temperatures than others. For instance, model GFDL-CM3 projected water temperatures slightly higher than the other ten models 19–43% of the time (Table 5A). Conversely, model NorESM1-ME tended to project temperatures that were lower than any other model 17–28% of the time (Table 5B). The small scale differences in projected temperatures are attributable to dissimilarities in the mechanics and complexity of each model (Flato et al., 2013). Among GFDL-CM3 and NorESM1-ME, for instance, the latter model includes components that were used to estimate terrestrial and marine carbon, features lacking in GFDL-CM3. For more information concerning the particular differences among the eleven models and how these affect their performance, see Flato et al. (2013).

3.3. Growth projections

The average of all 11 model simulations was used as the composite input variable in the growth vs. temperature equations for each species. Compositing was done because of the similarity among the modeled temperatures (and therefore high level of confidence in the projections) and to simplify the forecasts of *Gambierdiscus* growth (Fig. 5). Daily composite water temperatures were then used to calculate monthly and yearly composite temperatures at each site in the GCR. Average monthly and yearly growth rates for each *Gambierdiscus* species were calculated using these composite temperatures. The resulting growth projections for the five CFP-associated dinoflagellate species were very different in the western Gulf of Mexico compared to those in more tropical locations in the eastern Gulf and Caribbean Sea. At buoys WGOM/N and WGOM/S, which were characterized by the lowest average water temperatures before 2013, the average annual growth rates of all five dinoflagellate species are projected to increase throughout the remainder of the 21st century (Fig. 6A). *Gambierdiscus belizeanus*, *G. caribaeus* and *F. ruetzleri* are projected to undergo the greatest increases in average growth rate at WGOM/N of 0.08–0.1 d⁻¹ between 2000 and 2099 (from 0.11 to 0.19 d⁻¹, 0.16 to 0.24 d⁻¹, 0.16 to 0.26 d⁻¹, respectively) (Fig. 6A). At the same site, *G. carolinianus* and *Gambierdiscus* ribotype 2 are expected to undergo increases of ~0.07 d⁻¹ over the same period (0.15 to 0.22 d⁻¹, 0.07 to 0.14 d⁻¹, respectively).

Farther offshore at buoy WGOM/S, a smaller rise in average annual water temperature is projected to prompt more modest growth rate increases of 0.04–0.06 d⁻¹ among *G. belizeanus*, *G. caribaeus*, and *F. ruetzleri* (Fig. 6B). Both *G. carolinianus* and *Gambierdiscus*

ribotype 2 are projected to undergo lesser increases in growth rate (~0.03 d⁻¹) through ~2080, after which growth rate is projected to remain relatively constant. This stabilization of the average annual growth rates of both species as temperatures rise is curious, as mean temperatures at WGOM/S are expected to reach ~27 °C by 2080 or so. These conditions should allow increasing rates of growth in all five species (Table 4). However, monthly water temperatures at this site are expected to reach 31 °C during the summer months after 2070 and approach 32 °C in the summer by 2099. Such high seasonal water temperatures exceed T_{opt} for *G. carolinianus* and *Gambierdiscus* ribotype 2 (23.5–30.0 °C and 24.5–30.1 °C, respectively; Table 4), limiting growth of these species during the summer and yielding constant average annual growth rates (Fig. 6B). The high summer temperatures have a lesser effect on *G. belizeanus*, *G. caribaeus* and *F. ruetzleri*, which have higher T_{opt} values (24.5–31.9 °C, Table 4).

Despite the location of EGOM (~26° N) in the Gulf of Mexico, water temperatures at this site bear more similarity to stations in the Caribbean Sea than to those in the western Gulf. This similarity is attributable to transport of Caribbean water into the Gulf via the Loop Current, making average temperatures at EGOM only slightly lower than those in the Caribbean Sea (Fig. 5). As a result, station EGOM and the three sites in the Caribbean Sea (YUCT, CCAR, ECAR) are projected to exhibit very similar growth rates among the dinoflagellate species. With T_{opt} values of 24.5–31.9 °C, *G. caribaeus* and *F. ruetzleri* are projected to exhibit very little change in growth rate (≤ 0.01 d⁻¹) at EGOM, CCAR and ECAR despite gradually increasing water temperatures (Figs. 6C, E and F). This relative constancy is attributable to (1) the balance between elevated growth rates as winter temperatures rise and depressed growth rates as temperatures climb during the summer, (2) tolerance to high water temperatures in these two species and, (3) the relatively small degree of seasonal temperature change in the Caribbean Sea. A very similar trend is expected in *G. belizeanus*, which has a slightly lower T_{opt} range (24.5–31.7 °C). At YUCT, the slightly higher water temperatures projected to occur through the end of the century are expected to prompt declining average annual growth rates in all five dinoflagellate species (Fig. 6D). This decline is projected to be most substantial in *Gambierdiscus* ribotype 2 and *G. carolinianus* (0.03 to 0.06 d⁻¹, Fig. 6D).

3.4. Seasonality

Comparison of the seasonal temperature cycles at each site with the thermal growth responses of the five dinoflagellate species indicates higher summer water temperatures will likely have a substantial impact on the assemblage at each site. Monthly mean temperatures at WGOM/N currently average 30.2 °C during August of each year, temperatures that are already $>T_{opt}$ for both *G. carolinianus* and *Gambierdiscus* ribotype 2 (Fig. 7A, Table 4). With the increase of >2 °C projected to occur in the western Gulf by the end of the century (Fig. 5A and B), water temperatures at WGOM/N are expected to be $>T_{opt}$ for these two species during a five month period from mid-May through mid-September of each year. Peak summer temperatures are even projected to approach or exceed the thermal growth limit of both *G. carolinianus* ($T_u = 32.5$ °C) and *Gambierdiscus* ribotype 2 ($T_u = 33.0$ °C) by the end of the century (Fig. 7A). Such high summer temperatures would tend to severely limit the growth of these low temperature species and may cause mortality. *G. belizeanus*, *G. caribaeus* and *F. ruetzleri* are also projected to be negatively affected by peak summer temperatures, but only after ~2070 when temperatures at WGOM/N are projected to exceed T_{opt} for these three species.

Winter minimum temperatures also limit growth of CFP-associated dinoflagellates in the Gulf of Mexico. Water temperatures currently reach an average of 14.5–14.7 °C in January and

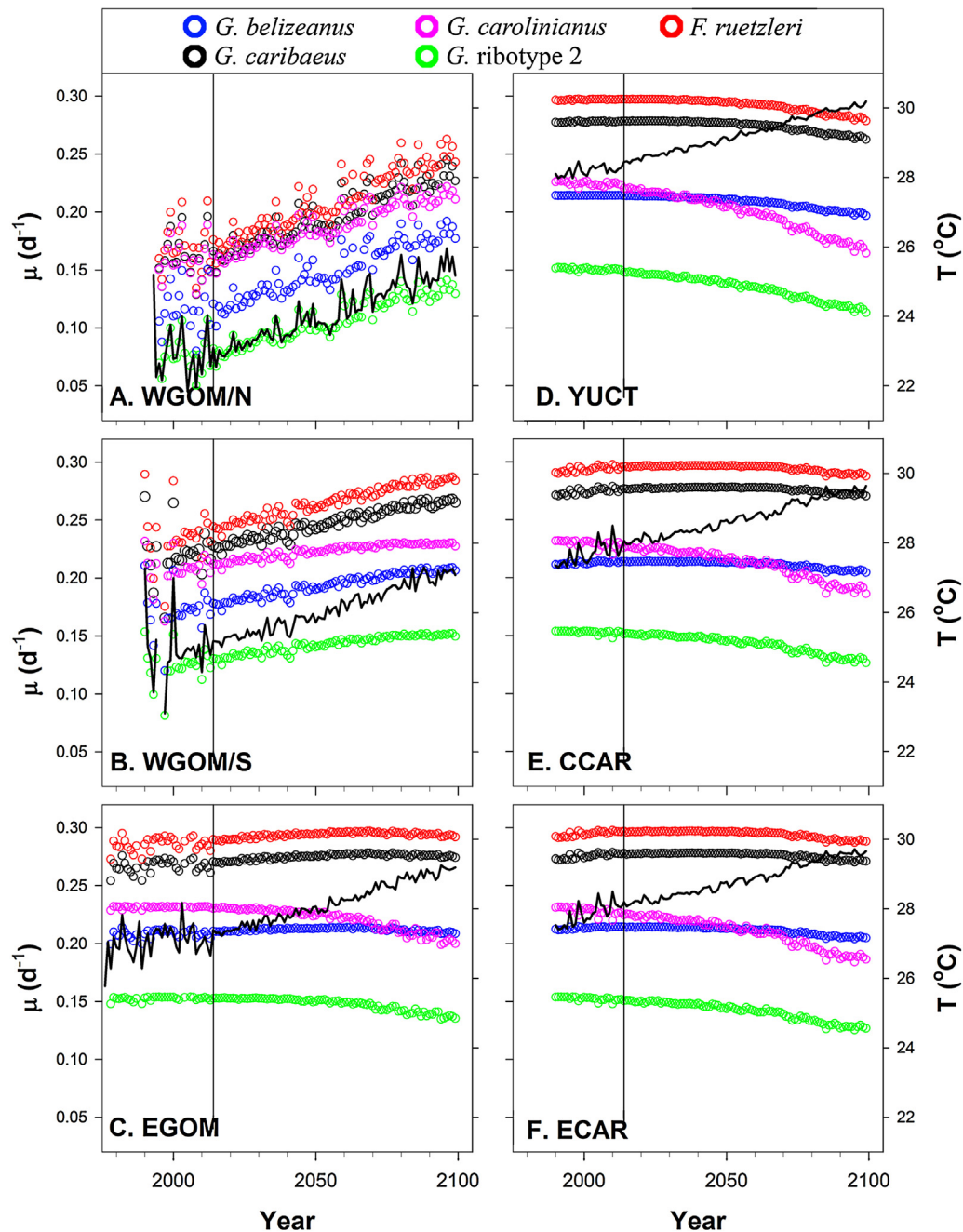


Fig. 6. Mean projected annual growth rates (open circles) and water temperature (solid line) for five CFP-associated dinoflagellate species at six stations in the Greater Caribbean region: *G. belizeanus* (blue circle), *G. caribaeus* (black circle), *G. carolinianus* (pink circle), *Fukuyoa ruetzleri* (red circle), *Gambierdiscus* ribotype 2 (green circle). Vertical reference lines denote the year 2013. (For interpretation of the references to color in this figure legend, the reader is referred to the web version of this article.)

February at WGOM/N. These temperatures are well below the thermal growth optima for all five dinoflagellate species during November–May, $<T_0$ for *G. belizeanus* and *Gambierdiscus* ribotype 2 during early November through mid-March, and $<T_0$ for the remaining species during December through mid-February (Fig. 7A). Low water temperatures are projected to prevent growth of these species during these periods. Despite warming conditions, winter water temperatures at this site are not expected to rise appreciably until the end of the century, when January–February temperatures are projected to reach to $\sim 17^{\circ}C$.

Located farther offshore, site WGOM/S is less affected by summer–winter temperature fluctuations than WGOM/N. As a result, peak summertime temperatures are currently within the T_{opt} range for all five dinoflagellate species, but are projected

to exceed the thermal optimum range of *G. carolinianus* and *Gambierdiscus* ribotype 2 after 2050 (Fig. 7B). Although summer temperatures are projected to reach $31.4^{\circ}C$ at this site by 2099, the hottest projected temperatures are still within T_{opt} for the high temperature species *G. belizeanus*, *G. caribaeus* and *F. ruetzleri* (Table 4). Like the inshore site WGOM/N, winter temperatures at WGOM/S are currently below the thermal optima for all Caribbean species during early December through mid-April, although this cold period is projected to shorten appreciably to only three months (January–March) by the end of the century (Fig. 7B). Only during February are current winter temperatures at WGOM/S $<T_0$ for any of the dinoflagellate species (*G. belizeanus*, $T_0 = 20.0^{\circ}C$, Table 4), but temperatures are expected to remain within the growth limits of all five species year round after 2050.

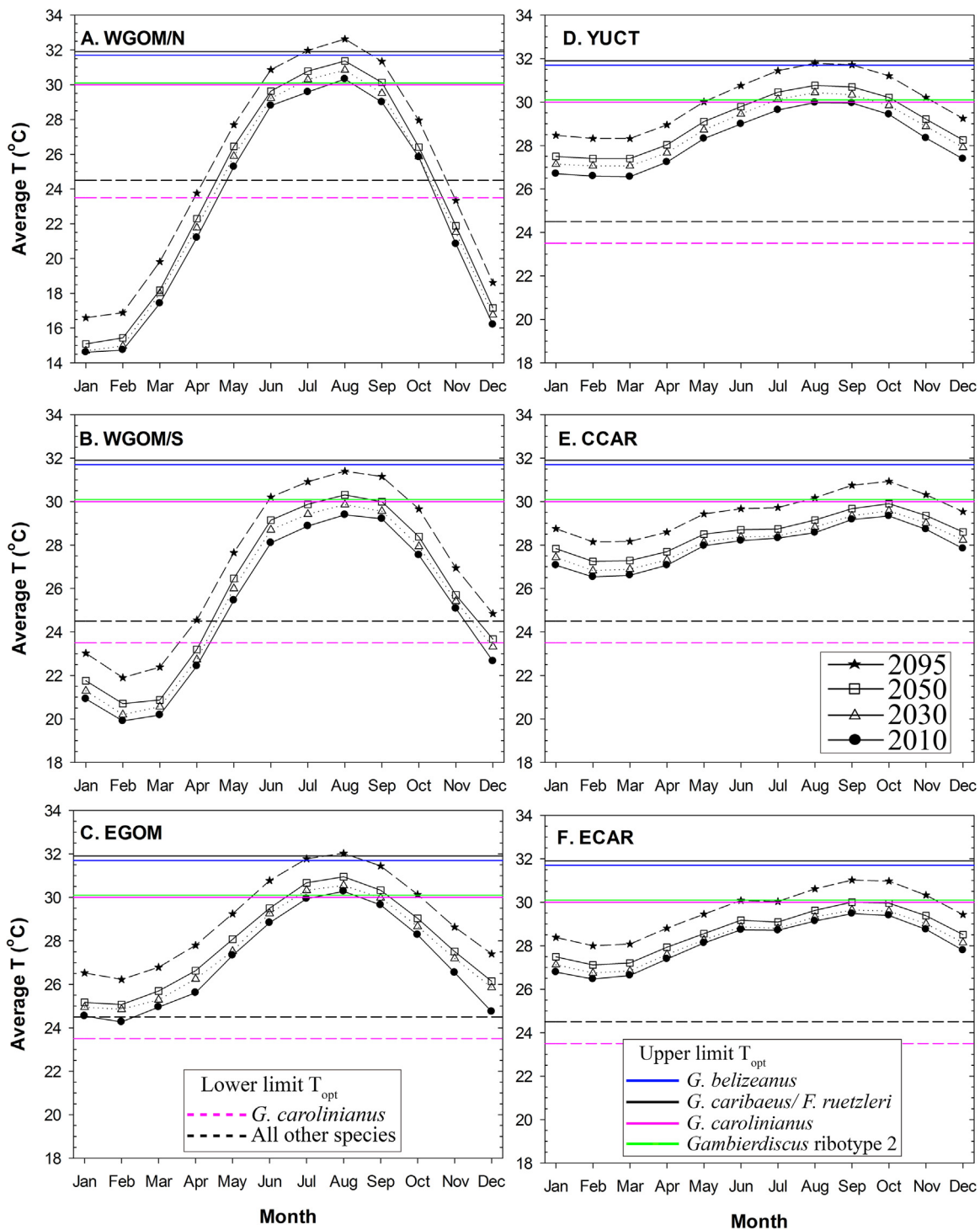


Fig. 7. Projected seasonal water temperatures at six locations in the Greater Caribbean region during four time periods: 2010 (2005–2014), 2030 (2025–2034), 2050 (2045–2054) and 2095 (2090–2099). Lateral solid lines denote the upper thermal limit for optimum growth ($\geq 80\% \mu_{max}$) for *G. belizeanus* (solid blue line), *Gambierdiscus caribaeus*/*F. ruetzleri* (solid black line), *G. carolinianus* (solid red line) and *Gambierdiscus* ribotype 2 (solid green line) (Table 4). Dashed lines denote the lower thermal limit for optimum growth in *G. carolinianus* (dashed red line) and in all other species (dashed black line). Note longer temperature scale in panel A. (For interpretation of the references to color in this figure legend, the reader is referred to the web version of this article.)

The seasonal cycle has an even smaller magnitude at EGOM and YUCT, where average temperatures fluctuate between 24.2 and 30.3°C (February, August) and 26.5–31.7°C (March, August), respectively (Fig. 7C and D). At EGOM, peak summer temperatures are currently high enough to limit growth rates of only *G. carolinianus* and *Gambierdiscus* ribotype 2, but are projected to affect the high temperature species as well by 2099. A similar trend is

expected to occur at YUCT, where summer temperatures are projected to begin limiting growth of *G. carolinianus* and *Gambierdiscus* ribotype 2 after ~2030 (Fig. 7D). During the winter, minimum water temperatures (26.5°C) are not low enough to limit optimum growth of any of the five dinoflagellates at YUCT, but may slightly limit the growth of all species except *G. carolinianus* in the eastern Gulf during February (Fig. 7C and D).

The Caribbean Sea sites CCAR and ECAR exhibit nearly identical seasonal temperature cycles characterized by peak water temperatures in September and October rather than the August high that occurs at the other four sites. CCAR and ECAR are also characterized by a bimodal seasonal temperature cycle with a noticeable mid-summer dip in water temperatures due to increasing wind and convective activity that is characteristic of the Caribbean Sea (e.g., Magaña et al., 1999). Summer temperatures average 29.3–29.5 °C at both CCAR and ECAR and are projected to remain within T_{opt} for all three of the high temperature species year round despite the steady regional rate of ocean warming. By 2099, peak summer water temperatures are projected to reach 30.9 °C and 31.0 °C at CCAR and ECAR (respectively), high enough to limit growth of *G. carolinianus* and *Gambierdiscus* ribotype 2 during July/August through November (Fig. 7E and F). Although summer temperatures would not likely be high enough to cause mortality, the net effect will be to suppress growth of *G. carolinianus* and *Gambierdiscus* ribotype 2 while stimulating the growth of warm tolerant species like *G. caribaeus* and *G. belizeanus*.

3.5. Optimum growth days

Projected water temperatures at each site and temperature vs. growth data made it possible to estimate the optimum growth days of each dinoflagellate species for the present-day, and how this number might change by the end of the 21st century. Optimum growth days (D_{opt}) were defined as the number of days per year (d yr^{-1}) when water temperatures were projected to lie within the optimum growth range (T_{opt} , $\geq 80\%$ maximum growth rate) for each dinoflagellate species (Table 4). Species tolerant of higher water temperatures—*G. caribaeus*/*F. ruetzleri* and *G. belizeanus*—were delineated by optimum days at or near 365 yr^{-1} at the three Caribbean Sea sites despite rising temperatures. Only at the end of the century are Caribbean Sea temperatures projected to be high enough to suppress the growth of these three species somewhat (YUCT, Fig. 8D). At station EGOM, sub-optimum conditions for growth of the three high temperature species are expected to persist during the winter months until after 2050, when D_{opt} is projected to reach 365 d yr^{-1} . As conditions in the eastern Gulf of Mexico continue to warm after ~ 2070 , summer temperatures are projected to exceed T_{opt} for *G. caribaeus*/*F. ruetzleri* and *G. belizeanus*, reducing the number of optimum days to near 300 d yr^{-1} (Fig. 8C).

In the western Gulf of Mexico, where water temperatures are somewhat lower and winter cooling is more intense (Figs. 5A and 7A), D_{opt} is projected to increase for the three high temperature species through at least 2060. D_{opt} values for *G. caribaeus*/*F. ruetzleri* and *G. belizeanus* are expected to decline again after ~ 2060 when summer temperatures begin to limit growth (Fig. 8A). At the offshore site WGOM/S, this upward trend is projected to continue through the remainder of this century (Fig. 8B).

The low temperature species, *G. carolinianus* and *Gambierdiscus* ribotype 2, are expected to experience an overall reduction in D_{opt} across the GCR by the end of the century, despite the projected increase in their average annual growth rates. The fewest optimum growth days for *G. carolinianus* and *Gambierdiscus* ribotype 2 currently occur at WGOM/N, where *Gambierdiscus* growth is limited by both winter temperatures $< T_{opt}$ and summer temperatures $> T_{opt}$ (Fig. 8A). For instance, daily water temperatures at WGOM/N during 2013 were $< T_{opt}$ for *G. carolinianus* ($< 23.5^\circ\text{C}$) for 195 d during the winter months and were $> T_{opt}$ for only 12 d during August and early September, leaving 158 d with optimum growth temperatures. By 2050, rising temperatures at this site are projected to reduce the number of suboptimal winter days to 173, but to increase the number of suboptimal summer days to 82. The net effect of these projected changes is an overall reduction in D_{opt} for *G. carolinianus* at WGOM/N to 110 d yr^{-1} by 2050 (Fig. 8A). By

the end of the century, D_{opt} is projected to decline even further to 102 d yr^{-1} for *G. carolinianus*, despite an overall increase in its projected annual average growth rate (Fig. 6A). This apparent contradiction of increasing annual growth rates (Fig. 6A and B) but decreasing optimum growth days (Fig. 8A and B) is attributable to much higher dinoflagellate growth rates during spring and fall, balanced by smaller decreases in growth during winter and summer. The net result is an overall increase in projected growth rates.

A similar pattern of declining optimum growth days yr^{-1} was projected for the low temperature species *G. carolinianus* and *Gambierdiscus* ribotype 2 at the offshore site WGOM/S, marked by a reduction from ~ 200 to $130\text{--}150 \text{ d yr}^{-1}$ by 2099 (Fig. 8B). Similarly, the even warmer, but more stable conditions in the eastern Gulf of Mexico are projected to prompt a decline in D_{opt} for these two species from $\sim 300 \text{ d yr}^{-1}$ at present to $\sim 225 \text{ d yr}^{-1}$ by the end of the century (Fig. 8C). The most dramatic decline in yearly optimum growth days for *G. carolinianus* and *Gambierdiscus* ribotype 2 is projected to occur at the Caribbean Sea sites, where optimum temperatures currently persist year round ($D_{opt} = 365 \text{ d yr}^{-1}$). As temperatures rise, the number of optimum growth days for these low temperature species are projected to decrease steadily after the middle of the century to $169\text{--}171 \text{ d yr}^{-1}$ at YUCT, to $228\text{--}252 \text{ d yr}^{-1}$ at CCAR, and to $187\text{--}199 \text{ d yr}^{-1}$ at ECAR (Fig. 8D–F).

4. Discussion

By the end of the 21st century, it is likely that diversity, abundance and distribution of CFP-associated dinoflagellate species will undergo significant changes based on temperature-growth models and projected ocean temperatures in the Greater Caribbean region (GCR). These changes are driven by the interactions between increasing water temperatures and the upper thermal growth limit (T_u), lower thermal growth limit (T_0), and thermal optimum growth range (T_{opt}) for each species (after Kibler et al., 2012). As temperatures rise, the effects will be most apparent on *G. carolinianus* and *Gambierdiscus* ribotype 2. These two species have growth optima of $\sim 24\text{--}30^\circ\text{C}$ and are better adapted to cooler temperatures, causing their prevalence in the Caribbean Sea to decline as temperatures increase. In contrast, because of their tolerance to cooler conditions it is projected these two species will become more abundant along the northern Gulf of Mexico and expand their ranges farther into the western Atlantic. Species tolerant of higher temperatures, such as *G. belizeanus*, *G. caribaeus* and *F. ruetzleri* ($T_{opt} \sim 24.5\text{--}31.9^\circ\text{C}$) are predicted to become increasingly dominant in the Caribbean Sea and surrounding areas. In the western Gulf of Mexico the abundance of CFP-associated species is limited by low temperatures for much of the year. During the months November through April water temperatures are below T_{opt} for all five species at WGOM/N and are $< T_{opt}$ during December–April at WGOM/S. The model results predict that as the water temperatures increase $2\text{--}4^\circ\text{C}$ this century all five of the dinoflagellate species in this study that co-occur in the Gulf are projected to increase in overall abundance, potentially increasing the risk of CFP.

4.1. Effects of seasonality

Differences in seasonal temperature fluctuations among the different GCR sites are most apparent in D_{opt} , which represents a balance between winter temperatures too low to support optimum dinoflagellate growth and summer temperatures too high for optimum growth. The greatest amount of seasonal water temperature change occurs in the temperate waters of the northwestern Gulf of Mexico (Fig. 7A and B), with a similar pattern along southeast U.S. Atlantic coast. In both locations, the severity of summer–winter temperature oscillation acts as a barrier to northward expansion

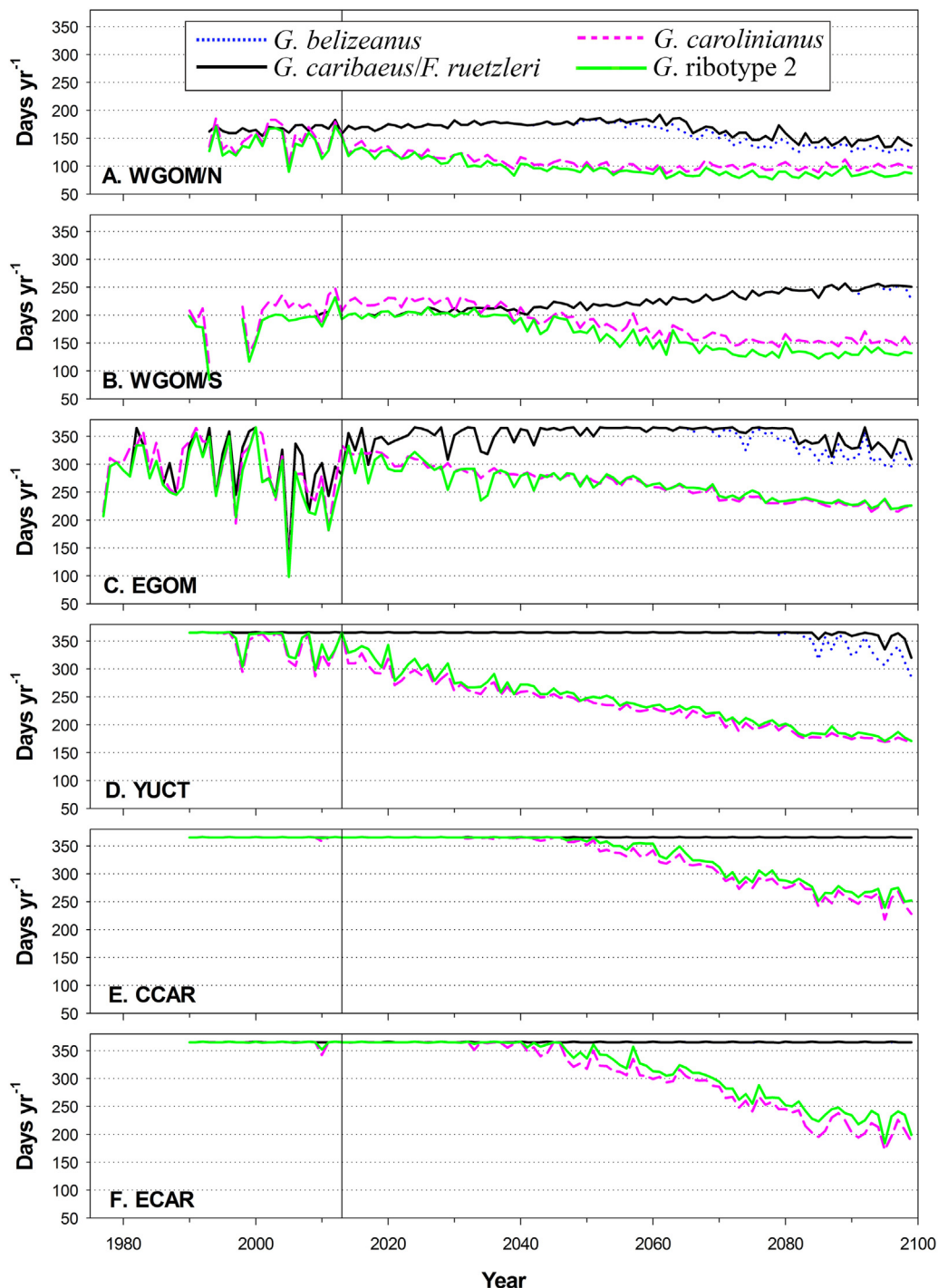


Fig. 8. Average number of days when water temperature allows optimum growth ($\geq 80\%$ maximum) at each station for five dinoflagellate species in the Caribbean region: *G. belizeanus* (dotted blue line), *Gambierdiscus caribaeus/F. ruetzleri* (solid black line), *G. carolinianus* (dashed red line) and *Gambierdiscus ribotype 2* (solid green line) (Table 4). Vertical reference lines denote the year 2013. (For interpretation of the references to color in this figure legend, the reader is referred to the web version of this article.)

of *Gambierdiscus* and *Fukuyoa* species. This barrier is reflected in the current distribution of CFP-associated dinoflagellates on the North Carolina continental shelf. The northward transport of cells in the Gulf Stream is a known mechanism for the introduction of dinoflagellates and other tropical biota into more temperate shelf environments, especially when temperatures are favorable during the summer (Bomber et al., 1988b; Faust and Tester, 2004; Thiel and Gutow, 2005). Those species best able to withstand low temperatures during the winter and reach optimum growth rates during the summer are expected to dominate the

CFP-associated dinoflagellate assemblage on the North Carolina shelf. This seasonal selection process accounts for the overall low *Gambierdiscus* and *Fukuyoa* abundance on the North Carolina shelf and the apparent dominance of the more cold-tolerant species *G. carolinianus* (W. Freshwater, unpublished data).

In the northwestern Gulf of Mexico, which lies $\sim 7^\circ$ further south than the North Carolina shelf, low winter temperatures have a similar effect on CFP-associated dinoflagellate abundance and diversity. Because of the low temperatures during the winter months, the growth season for these dinoflagellates in the northwestern Gulf is

limited to May–October when water temperatures are within T_{opt} for each of the dinoflagellate species (Fig. 7). At station WGOM/N, inshore water temperatures average $\sim 14^\circ\text{C}$ in January–February and reach $\sim 30^\circ\text{C}$ during July–August (Fig. 7A). A more moderate seasonal pattern occurs further offshore at station WGOM/S, where temperatures vary between 19 and 29°C (Fig. 7B). The greater seasonal variation and terrestrial runoff at inshore locations likely prevents *Gambierdiscus* and *Fukuyoa* species from reaching high abundances. This likelihood is supported by Tester et al. (2013), who showed the five dinoflagellate species examined here occurred at East and West Flower Garden Banks (~ 200 km offshore), but that lower wintertime temperatures at Stetson Bank, an inshore site located just 130 km off from the coast, probably limited the occurrence of these species. A subsequent survey for CFP-associated dinoflagellates in 2013 confirmed only *G. carolinianus* was present at Stetson Bank (W. Litaker, unpublished data).

The seasonal temperature cycle has a more moderate effect on water temperatures in other portions of the GCR. In the eastern Gulf of Mexico, Yucatan coastal region and northwestern Caribbean Sea, where the annual water temperature range is $\sim 6^\circ\text{C}$ (24 – 30°C at EGOM) and $\sim 3.5^\circ\text{C}$ (26.5 – 30°C at YUCT), water temperatures almost never dip below T_{opt} for the five dinoflagellates. As a result, temperatures are warm enough to support optimum growth from March to early December in the eastern Gulf and year round in the western Caribbean Sea (Fig. 7C and D). This pattern is not projected to change at either site through the end of the century. Instead, the main seasonal limitation on dinoflagellate growth in the Caribbean Sea will be during mid-summer, when suboptimally high temperatures are projected to restrict growth of some species. As a result, it is likely the CFP dinoflagellate assemblage will be dominated by *G. belizeanus*, *G. caribaeus* and *F. ruetzleri* during the summer, while all five species will attain optimum growth rates during the remainder of the year. In the central and eastern Caribbean Sea, where seasonal temperature differences are smallest ($\sim 1.5^\circ\text{C}$ at CCAR and ECAR), the long term warming trend will likely have a more substantial effect on dinoflagellate growth, diversity and distribution.

Seasonal cycles of *Gambierdiscus* abundance have been recognized as a factor driving temporal variability in CFP occurrence worldwide. Carlson and Tindall (1985), Gillespie et al. (1985a, 1985b), Taylor (1985) and Hurbungs et al. (2001) each characterized seasonal occurrence of CFP, but were unable to pinpoint the causative factors. In the GCR, the seasonality of temperature-growth effects on *Gambierdiscus* abundance are potentially complicated by other seasonal signals including variation in the timing of dry vs. rainy seasons and seasonal wind-driven upwelling (Curtis and Gamble, 2007; Gamble and Curtis, 2008; Gamble et al., 2008; Carrillo et al., 2009). Some of these effects occur at relatively small spatial scales, such as the upwelling along the east coast of Florida, USA, southern Gulf of Mexico and the Atlantic coast of Colombia and Venezuela (Leming and Mooers, 1981; Pitts, 1993; Andrade and Barton, 2005; Zavala-Hidalgo et al., 2006; Lonin et al., 2010). As a result, localized meteorological drivers may be much more important in these locations, rendering seasonal changes in CFP dinoflagellate occurrence more difficult to predict.

4.2. Bloom development and CFP risk

Projected growth data from this study were used to predict the occurrence of *Gambierdiscus* and *Fukuyoa* species in different parts of the GCR, but may also provide information about abundance of each species and its potential contribution to CFP. Unlike many planktonic harmful algal bloom dinoflagellates that grow rapidly (0.5 – 3 d^{-1}) and form surface blooms (Smayda, 1997; Garcés et al., 1999), *Gambierdiscus* and *Fukuyoa* species are relatively large ($>50\text{ }\mu\text{m}$) and typically exhibit low division rates (0.1 – 0.2 d^{-1}) (Bomber et al., 1988a; Morton et al., 1992; Litaker et al., 2009;

Kibler et al., 2012). *Gambierdiscus* cells are also predominantly benthic, commonly occurring in coral reef and seagrass systems at low abundances (1 – 10 cells g^{-1}) on a variety of substrates including macrophytes, dead corals, and other surfaces (Litaker et al., 2010). In these oligotrophic/mesotrophic environments, *Gambierdiscus* and *Fukuyoa* blooms develop slowly and several months may be required for cells to reach the high abundances seemingly necessary for CFP outbreaks (Taylor and Gustavson, 1985; Chinain et al., 1999; Chateau-Degat et al., 2005). At a bloom abundance threshold of $\sim 1000\text{ cells g}^{-1}$ substrate, the likelihood of CFP toxins accumulating in the marine food web increases substantially (Litaker et al., 2010). The amount of time necessary for such blooms to occur may be approximated using a simple growth rate equation of the form $\mu = \ln(C_1/C_2)/\Delta t$, where μ represents the daily growth rate (d^{-1}), C_1 and C_2 are the initial and final cell abundances (cells g^{-1}), and Δt denotes time elapsed (days, d). For a species such as *G. caribaeus*, which is widely distributed over the Caribbean region, the maximum growth rate at a moderate water temperature of 25 – 26°C is expected to be ~ 0.23 to 0.24 d^{-1} (Fig. 4B). At such growth rates, approximately one month is required for a background level of abundance of 1 cell g^{-1} substrate to develop into a bloom of 1000 cells g^{-1} . Previous work has shown a 1–2 month incubation period is realistic for *Gambierdiscus* and *Fukuyoa* blooms to develop, although a 3–4 month period is more common considering potential loss of *Gambierdiscus* cells from advection, grazing and competition with other metaflora (Ballantine et al., 1988; Chinain et al., 1999). As water temperatures approach 30°C through the latter half of this century, the incubation period required to form the same bloom will be shortened to 24–25 days. Alternatively, the same one month incubation period would allow a more substantial bloom of 4000 – 5000 cells g^{-1} to develop.

Based on these estimates, it is clear that both temperature and incubation time of *Gambierdiscus* cells are critical components in the predictability of blooms and subsequent risk of CFP outbreaks. Where the temperatures are too low, or where the window for optimal growth is too short, cell biomass will be insufficient to allow large amounts of CTXs to accumulate in the food web and CFP risk will remain low. In the GCR this low risk region currently includes the temperate waters between approximately Cape Canaveral, Florida (28.45°N) and Cape Hatteras, North Carolina (35.22°N). Further to the south between Cape Canaveral and the northern coast of Yucatan peninsula, subtropical conditions prevail and water temperatures are high enough for optimum *Gambierdiscus* growth rates during a 3–5 month summer growing season (June–October). Within these latitudes, *Gambierdiscus* abundance may reach high enough concentrations in summer to substantially increase the risk of CTX accumulation in marine fish and invertebrates. Given the lag between *Gambierdiscus* and *Fukuyoa* blooms and subsequent toxicity in fishes (Ballantine et al., 1988), the highest risk of CFP should occur in the later summer through autumn period (August–November). In the tropical region from the northern Yucatan to the north coast of South America, where optimum growth conditions persist through the winter months, mid-summer water temperatures likely depress *Gambierdiscus* and *Fukuyoa* growth rates. As a result, growth and abundance of these species is expected to be highest during the spring and autumn months (April–June, September–December) and the highest CFP risks will follow in July–September and January–March. This bimodality of *Gambierdiscus* growth, combined with uncertainty about the lag necessary for CTX accumulation, greatly complicates prediction of seasonal CFP occurrence in much of the Caribbean. Such complexity may account for the conflicting results about seasonal trends in CFP occurrence (Ballantine et al., 1985, 1988; Bomber, 1987; Tosteson et al., 1988; Tosteson, 2004; Tester et al., 2010; Radke et al., 2013; Gingold et al., 2014). The projected increase in water temperatures across the GCR is expected to fur-

ther complicate local CFP prediction in much of the Caribbean proper by lengthening the suboptimally warm period during mid-summer and by shifting the peak growing seasons toward February–April and November–December. As a result, portions of the year previously identified by local knowledge as having high CFP risk may change markedly. Given the degree to which water temperatures in the GCR have already changed over the last two decades (Fig. 5), changes in spatial and seasonal patterns of local CFP occurrence are likely already underway (e.g., Tosteson, 2004).

The RCP6.0 scenario used in this study to project ocean temperatures is one of four greenhouse gas concentration trajectories (RCP2.6, RCP4.5, RCP6.0, RCP8.5) that describe different climate futures for the Earth based on assumptions about economic activity, energy sources, human population growth and other social and economic factors (IPCC, 2013). RCP6.0 assumes that global annual greenhouse gas emissions will reach a maximum around 2080, yielding a mean surface temperature rise of 1.3 °C by mid-century and 2.2 °C by 2100 (IPCC, 2013, Table SPM.2). In contrast, RPCs 2.6 and 4.5 are expected to yield more modest average temperature increases of 1.0 °C and 1.8 °C by 2100, while RCP8.5 predicts a larger increase of 3.7 °C over the same period. In this study, RPC6.0 was selected to generate water temperature projections at the six locations in the GCR because it utilizes an intermediate greenhouse gas emission scenario (among other factors) in comparison to RPCs 2.6, 4.5 and 8.5 (Meinshausen et al., 2011). Because the models used in this study relate changes to temperature alone, the differences among different RCP scenarios would be primarily a matter of the timing of the changes, as sea surface temperatures closely follow changes in global temperature. Analysis of the characteristics and relative uncertainties of each RCP is beyond the scope of this study, but the relatively narrow 95% confidence bounds among the different temperature models (Fig. 5) indicate a clear warming trend at each site. Given that global fossil fuel emissions have not been appreciably reduced as of 2015 (e.g., Burck et al., 2015), our selection of RCP6.0 seems realistic when compared with those scenarios that assume more rapid stabilization of emission levels (RPC2.4, RPC4.5). For more information about each RCP, the reader is directed to other sources (e.g., Meinshausen et al., 2011; IPCC, 2013).

5. Conclusions

The growth and abundance of *Gambierdiscus* and *Fukuyoa* species in the Gulf of Mexico are expected to change in response to higher temperatures, although the response of individual species depends on the location. In the more temperate portions of the northern Gulf and the U.S. southeast Atlantic coast, the abundance of all *Gambierdiscus* and *Fukuyoa* species is projected to increase with higher average growth rates. Species such as *G. carolinianus* and *Gambierdiscus* ribotype 2, which are tolerant of lower water temperatures, are expected to undergo range expansions northward as the ocean warms. Where water temperatures are higher in the eastern Gulf of Mexico and Caribbean Sea, warm-tolerant species like *G. belizeanus*, *G. caribaeus* and *F. ruetzleri* will become increasingly dominant. This prediction does not necessarily mean species with lower thermal tolerances will be unable to survive in the Caribbean Sea, but that these species will be less prevalent.

The projected changes in growth and abundance of ciguatera-associated dinoflagellates will prompt gradual shifts in CFP risk in the coming decades. Higher incidences are likely in the Gulf of Mexico and U.S. southeast Atlantic coast. Stable or slightly declining CFP incidences are expected in the Caribbean Sea. The degree to which CFP risks will change depends largely on the toxicity of each dinoflagellate species. Only when the toxicity of each has been fully characterized can these data be combined with the projec-

tions from this study to inform CFP risk assessments for the Greater Caribbean region.

Acknowledgements

We wish to extend our thanks to D. Hardison and W. Holland for assistance with experimental data, internal reviewers at the Beaufort Laboratory and Center the Northwest Fisheries Science Center for helpful comments that greatly improved the manuscript; and to J. Trtanj, M. Faust and UNESCO/IOC/SCOR's Program on HABs in Benthic Systems (GEOHAB) for inspiration. Funding for this work was provided by The National Centers for Coastal Ocean Science, NOAA.

The views expressed herein are those of the authors and do not necessarily reflect the views of NOAA or any of its subagencies. Mention of trade names or commercial products does not constitute endorsement or recommendation for their use by the United States government.

References

- Andrade, C.A., Barton, E.D., 2005. The Guajira upwelling system. *Cont. Shelf Res.* 25, 1003–1022. <http://dx.doi.org/10.1016/j.csr.2004.12.012>.
- Bagnis, R., Bennett, J., Prieur, C., Legrand, A.M., 1985. The dynamics of three toxic benthic dinoflagellates and the toxicity of ciguatera surgeonfish in French Polynesia. In: Anderson, D.M., White, A.W., Baden, D.G. (Eds.), *Toxic Dinoflagellates*. Elsevier, New York, pp. 177–182.
- Bagnis, R., Chanteau, S., Chungue, E., Hurtel, J.M., Yasumoto, T., Inoue, A., 1980. Origins of ciguatera fish poisoning: a new dinoflagellate, *Gambierdiscus toxicus* Adachi and Fukuyo, definitively involved as a causal agent. *Toxicon* 18, 199–208. [http://dx.doi.org/10.1016/0041-0101\(80\)90074-4](http://dx.doi.org/10.1016/0041-0101(80)90074-4).
- Ballantine, D.L., Bardales, A.T., Tosteson, T.E., Dupont-Durst, H., 1985. Seasonal abundance of *Gambierdiscus toxicus* and *Ostreopsis* sp. in coastal waters of southwest Puerto Rico. In: Gabrie, C., Salvat, B. (Eds.), *Proceedings of the 5th International Coral Reef Congress*, vol. 4. Antenne Museum-EPHE, Tahiti, pp. 417–422.
- Ballantine, D.L., Tosteson, T.R., Bardales, A.T., 1988. Population dynamics and toxicity of natural populations of benthic dinoflagellates in southwest Puerto Rico. *J. Exp. Mar. Biol. Ecol.* 119, 201–212.
- Bomber, J.W., (M.S. thesis) 1987. Ecology, Genetic Variability, and Physiology of the Ciguatera-causing Dinoflagellate *Gambierdiscus toxicus* Adachi & Fukuyo (Florida Keys, Caribbean). Florida Institute of Technology, Melbourne, FL.
- Bomber, J.W., Guillard, R.R.L., Nelson, W.G., 1988a. Roles of temperature, salinity, and light in seasonality, growth, and toxicity of ciguatera-causing *Gambierdiscus toxicus* Adachi et Fukuyo (Dinophyceae). *J. Exp. Mar. Biol. Ecol.* 115, 53–65.
- Bomber, J.W., Morton, S.L., Babinchak, J.A., Norris, D.R., Morton, J.G., 1988b. Epiphytic dinoflagellates of drift algae—another toxigenic community in the ciguatera food chain. *Bull. Mar. Sci.* 43, 204–214.
- Bomber, J.W., Tindall, D.R., Miller, D.M., 1989. Genetic variability in toxin potencies in seventeen clones of *Gambierdiscus toxicus* (Dinophyceae). *J. Phycol.* 25, 617–625. <http://dx.doi.org/10.1111/j.0022-3646.1989.00617.x>.
- Burck, J., Marten, F., Bals, C., 2015. The Climate Change Performance Index Results 2015. Germanwatch e.v., Bonn. (accessed 23.07.15) <http://www.germanwatch.org/en/ccpi>.
- Carlson, R.D., (Ph.D. dissertation) 1984. Distribution, periodicity and culture of benthic/epiphytic dinoflagellates in a ciguatera endemic region of the Caribbean. Department of Botany in the Graduate School, Southern Illinois University at Carbondale, Carbondale, IL.
- Carlson, R.D., Tindall, D.R., 1985. Distribution and periodicity of toxic dinoflagellates in the Virgin Islands. In: Anderson, D.M., White, A.W., Baden, D.G. (Eds.), *Toxic Dinoflagellates*. Elsevier, New York, pp. 171–176.
- Carrillo, L., Palacios-Hernández, E., Yescas, M., Ramírez-Manguilar, A.M., 2009. Spatial and seasonal patterns of salinity in a large and shallow tropical estuary of the western Caribbean. *Estuaries Coasts* 32, 906–916. <http://dx.doi.org/10.1007/s12237-009-9196-2>.
- Chateau-Degat, M.-L., Chinain, M., Cerf, N., Gingrass, S., Hubert, B., Dewailly, E., 2005. Seawater temperature, *Gambierdiscus* spp. variability and incidence of ciguatera poisoning in French Polynesia. *Harmful Algae* 4, 1053–1062. <http://dx.doi.org/10.1016/j.hal.2005.03.003>.
- Chinain, M., Darius, H.T., Ung, A., Fouc, M.T., Revel, T., Cruchet, P., Pauillac, S., Laurent, D., 2010. Ciguatera risk management in French Polynesia: the case study of Raivavae Island (Australes Archipelago). *Toxicon* 56, 674–690. <http://dx.doi.org/10.1016/j.toxicon.2009.05.032>.
- Chinain, M., Germain, M., Deparis, X., Pauillac, S., Legrand, A.M., 1999. Seasonal abundance and toxicity of the dinoflagellate *Gambierdiscus* sp. (Dinophyceae), the causative agent of ciguatera in Tahiti, French Polynesia. *Mar. Biol.* 135, 259–267. <http://dx.doi.org/10.1007/s002270050623>.
- Chollett, I., Müller-Karger, F.E., Heron, S.F., Skirving, W., Mumby, P.J., 2012. Seasonal and spatial heterogeneity of recent sea surface temperature trends in the Caribbean Sea and southeast Gulf of Mexico. *Mar. Poll. Bull.* 64, 956–965. <http://dx.doi.org/10.1016/j.marpolbul.2012.02.016>.

- Curtis, S., Gamble, D.W., 2007. Regional variations of the Caribbean mid-summer drought. *Theor. Appl. Climatol.* 94, 25–34, <http://dx.doi.org/10.1007/s00704-007-0342-0>.
- Faust, M.A., Litaker, R.W., Vandersea, M.W., Kibler, S.R., Tester, P.A., 2005. Dinoflagellate diversity and abundance in two Belizean coral-reef mangrove lagoons: a test of Margalef's Mandala. *Atoll Res. Bull.* 534, 103–131.
- Faust, M.A., Tester, P.A., 2004. Harmful dinoflagellates in the Gulf Stream and Atlantic barrier coral reef, Belize. In: Steidinger, K.A., Lansberg, J.H., Tomas, C.R., Vargo, G.A. (Eds.), *Harmful Algae 2002. Proceedings of the 10th International Conference on Harmful Algal Blooms*, St. Pete Beach, FL, 21–25 October 2002. Florida Marine Research Institute, Florida Fish and Wildlife Conservation Commission, Florida Institute of Oceanography, Intergovernmental Oceanographic Commission of UNESCO, St. Petersburg, FL, pp. 326–328.
- Flato, G., Marotzke, J., Abiodun, B., Braconnot, P., Chou, S.C., Collins, W., Cox, P., Driouch, F., Emori, S., Eyring, V., Forest, C., Gleckler, P., Guilyardi, E., Jakob, C., Kattsov, V., Reason, C., Rummukainen, M., 2013. Evaluation of climate model. In: Stocker, T.F., Qin, D., Plattner, G.K., Tignor, M., Allen, S.K., Boschung, J., Nauels, A., Xia, Y., Bex, V., Midgley, P.M. (Eds.), *Climate Change 2013: The Physical Science Basis, Contribution of Working Group I to the Fifth Assessment Report of the Intergovernmental Panel on Climate Change*. Cambridge University Press, New York, pp. 741–866.
- Gallegos, A., 1996. Descriptive physical oceanography of the Caribbean Sea. In: Maul, G.A. (Ed.), *Small Islands: Marine Science and Sustainable Development*. American Geophysical Union, Washington, DC, pp. 36–55, <http://dx.doi.org/10.1029/CE051p0036>.
- Gamble, D.G., Curtis, S., 2008. Caribbean precipitation: review, model and prospect. *Progr. Phys. Geogr.* 32, 265–276, <http://dx.doi.org/10.1177/0309133308096027>.
- Gamble, D.G., Parnell, D.B., Curtis, S., 2008. Spatial variability of the Caribbean mid-summer drought and relation to north Atlantic high circulation. *Int. J. Climatol.* 28, 343–350, <http://dx.doi.org/10.1002/joc.1600>.
- Garcés, E., Delgado, M., Masó, M., Camp, J., 1999. In situ growth rate and distribution of the ichthyotoxic dinoflagellate *Gyrodinium corsicum* Paulmier in an estuarine embayment (Alfacs Bay, NW Mediterranean Sea). *J. Plankton Res.* 21, 1977–1991, <http://dx.doi.org/10.1093/plankt/21.10.1977>.
- GEOHAB, 2012. Global ecology and oceanography of harmful algal blooms, GEOHAB core research project: HABs in benthic systems. In: Berdalet, E., Tester, P., Zingone, A. (Eds.), *IOC of UNESCO and SCOR, Paris*. (accessed 19.05.15) http://www.ioc-unesco.org/hab/index.php?option=com_oe&task=viewDocumentRecord&docID=9693.
- Gillespie, N., Holmes, M.J., Burke, J.B., Doley, J., 1985a. Distribution and periodicity of *Gambierdiscus toxicus* in Queensland Australia. In: Anderson, D.M., White, A.W., Baden, D.G. (Eds.), *Toxic Dinoflagellates*. Elsevier, New York, pp. 183–188.
- Gillespie, N., Lewis, R., Burke, J., Holmes, M., 1985b. The significance of the absence of ciguatera toxin in a wild population of *G. toxicus*. In: Gabrie, C., Salvat, B. (Eds.), *Proceedings of the 5th International Coral Reef Congress*. Antenne Museum-EPHE, Tahiti, pp. 437–442.
- Gingold, D.B., Strickland, M.J., Hess, J.J., 2014. Ciguatera fish poisoning and climate change: analysis of National Poison Control Center data in the United States, 2001–2011. *Environ. Health Perspect.* 122, 580–586, <http://dx.doi.org/10.1289/ehp.1307196>.
- Gledhill, D.K., Wanninkhof, R., Millero, F.J., Eakin, M., 2008. Ocean acidification of the Greater Caribbean Region 1996–2006. *J. Geophys. Res. Oceans* 113, C10031, <http://dx.doi.org/10.1029/2007JC004629>.
- Gómez, F., Qiu, D., Lopes, R.M., Lin, S., 2015. *Fukuyoa paulensis* gen. et sp. nov., a new genus for the globular species of the dinoflagellate *Gambierdiscus* (Dinophyceae). *PLOS ONE* 10, e0119676, <http://dx.doi.org/10.1371/journal.pone.0119676>.
- Good, S.A., Corlett, G.K., Remedios, J.J., Noyes, E.J., Llewellyn-Jones, D.T., 2007. The global trend in sea surface temperature from 20 years of advanced very high resolution radiometer data. *J. Climatol.* 20, 1255–1264, <http://dx.doi.org/10.1175/JCLI4049.1>.
- Gordon, A.L., 1967. Circulation of the Caribbean Sea. *J. Geophys. Res.* 72, 6207–6223, <http://dx.doi.org/10.1029/JZ072i024p06207>.
- Hales, S., Weinstein, P., Woodward, A., 1999. Ciguatera (fish poisoning), El Niño, and Pacific sea surface temperatures. *Ecosys. Health* 5, 20–25, <http://dx.doi.org/10.1046/j.1526-0992.1999.09903.x>.
- Hoegh-Guldberg, O., Bruno, J., 2010. The impact of climate change on the world's marine ecosystems. *Science* 328, 1523, <http://dx.doi.org/10.1126/science.1189930>.
- Hurbungs, M.D., Jayabalan, N., Chineah, V., 2001. Seasonal distribution of potentially toxic benthic dinoflagellates in the lagoon of Trou Aux Biches, Mauritius. In: Lalouette, J.A., Bachraz, D.Y. (Eds.), *Proceedings of the Fifth Annual Meeting of Agricultural Scientists, Food and Agricultural Research Council*. Reduit, Mauritius, pp. 211–217.
- IPCC, 2013. *Climate change 2013: the physical science basis*. In: Stocker, T.F., Qin, D., Plattner, G.-K., Tignor, M., Allen, S.K., Boschung, J., Nauels, A., Xia, Y., Bex, V., Midgley, P.M. (Eds.), *Contribution of Working Group I to the Fifth Assessment Report of the Intergovernmental Panel on Climate Change*. Cambridge University Press, Cambridge, p. 1535 pp.
- Kibler, S.R., Litaker, R.W., Holland, W.C., Vandersea, M.W., Tester, P.A., 2012. Growth of eight *Gambierdiscus* (Dinophyceae) species: effects of temperature, salinity and irradiance. *Harmful Algae* 19, 1–14, <http://dx.doi.org/10.1016/j.hal.2012.04.007>.
- Kleypas, J.A., Danabasoglu, G., Lough, J.M., 2008. Potential role of the ocean thermostat in determining regional differences in coral reef bleaching events. *Geophys. Res. Lett.* 35, L03613, <http://dx.doi.org/10.1029/2007GL032257>.
- Lartigue, J., Jester, E.L.E., Dickey, R.W., Villareal, T.A., 2009. Nitrogen source effects on the growth and toxicity of two strains of the ciguatera causing dinoflagellate *Gambierdiscus toxicus*. *Harmful Algae* 8, 781–791, <http://dx.doi.org/10.1016/j.hal.2008.05.006>.
- Leming, T.D., Mooers, C.N.K., 1981. Cold water intrusions and upwelling near Cape Canaveral, Florida. In: Richards, F.A. (Ed.), *Coastal Upwelling*. American Geophysical Union, Washington, DC, <http://dx.doi.org/10.1029/C0001p0063>.
- Litaker, R.W., Vandersea, M.W., Faust, M.A., Kibler, S.R., Chinain, M., Holmes, M.J., Holland, W.C., Tester, P.A., 2009. Taxonomy of *Gambierdiscus* including four new species, *Gambierdiscus caribaeus*, *Gambierdiscus carolinianus*, *Gambierdiscus carpenteri* and *Gambierdiscus ruetzleri* (Gonyaulacales, Dinophyceae). *Phycologia* 48, 344–390, <http://dx.doi.org/10.2216/07-15.1>.
- Litaker, R.W., Vandersea, M.W., Faust, M.A., Kibler, S.R., Nau, A.W., Holland, W.C., Chinain, M., Holmes, M.J., Tester, P.A., 2010. Global distribution of ciguatera causing dinoflagellates in the genus *Gambierdiscus*. *Toxicon* 56, 711–730, <http://dx.doi.org/10.1016/j.toxicon.2010.05.017>.
- Llewellyn, L.E., 2010. Revisiting the association between sea surface temperature and the epidemiology of fish poisoning in the South Pacific: reassessing the link between ciguatera and climate change. *Toxicon* 56, 691–697, <http://dx.doi.org/10.1016/j.toxicon.2009.08.011>.
- Lonin, S.A., Hernández, J.L., Palacios, D.M., 2010. Atmospheric events disrupt coastal upwelling in the southwestern Caribbean. *J. Geophys. Res. Oceans* 115, C06030, <http://dx.doi.org/10.1029/2008JC005100>.
- Magaña, V., Amador, J.A., Medina, S., 1999. The midsummer drought over Mexico and Central America. *J. Climate* 12, 1577–1588.
- Meinshausen, M., Smith, S.J., Calvin, K., Daniel, J.S., Kainuma, M.L.T., Lamarque, J.-F., Matsumoto, K., Montzka, S.A., Raper, S.C.B., Riahi, K., Thomson, A., Velders, G.J.M., van Vuuren, D.P.P., 2011. The RCP greenhouse gas concentrations and their extensions from 1765 to 2300. *Clim. Chang.* 109, 213–241.
- Morton, S.L., Norris, D.R., Bomber, J.W., 1992. Effect of temperature, salinity and light intensity on the growth and seasonality of toxic dinoflagellates associated with ciguatera. *J. Exp. Mar. Biol. Ecol.* 157, 79–90, [http://dx.doi.org/10.1016/0022-0981\(92\)90076-M](http://dx.doi.org/10.1016/0022-0981(92)90076-M).
- Nascimento, S.M., Monteiro, P.O., Alencar, A.G., Meneguelli, A.C., 2010. Epibenthic dinoflagellates from the Rio de Janeiro coastline, Brazil. In: GEOHAB Open Science Meeting on the Core Research Project: HABs in Benthic Systems, Honolulu, Hawaii, U.S.A., UNESCO-IOC SCOR, 21–23 June 2010. Program Book, p. 30, Available from: <http://www.scor-int.org/GEOHAB.BHAB.Program.Book.pdf> (accessed 20.05.15).
- National Centers for Environmental Information (NCEI), 2015. Extended Reconstructed Sea Surface Temperature (ERSST) v3b. National Oceanic and Atmospheric Administration (accessed 19.05.15) <http://www.ncdc.noaa.gov/data-access/marineocean-data/extended-reconstructed-sea-surface-temperature-ersst-v3b>.
- National Data Buoy Center (NDBC), 2015. National Data Buoy Center Mapviewer. National Oceanic and Atmospheric Administration (accessed 19.05.15) <http://www.ndbc.noaa.gov>.
- Nishimura, T., Sato, S., Tawong, W., Sakanari, H., Uehara, K., Rhamam Shah, M.M., Suda, S., Yasumoto, T., Taira, Y., Yamaguchi, H., Adachi, M., 2013. Genetic diversity and distribution of the ciguatera-causing dinoflagellate *Gambierdiscus* spp. (Dinophyceae) in coastal areas of Japan. *PLOS ONE* 8, e60882, <http://dx.doi.org/10.1371/journal.pone.0060882>.
- Nishimura, T., Sato, S., Tawong, W., Sakanari, H., Yamaguchi, H., Adachi, M., 2014. Morphology of *Gambierdiscus scabrosus* sp. nov. (Gonyaulacales): a new epiphytic toxic dinoflagellate from coastal areas of Japan. *J. Phycol.* 50, 506–514, <http://dx.doi.org/10.1111/jpy.12175>.
- Okolodkov, Y.B., del Carmen Merino-Virgilio, F., Antolín Aké-Castillo, J., Concepción Aguilar-Trujillo, A., Espinosa-Matías, S., Herrera-Silveira, A., 2014. Seasonal changes in epiphytic dinoflagellate assemblages near the northern coast of the Yucatan Peninsula, Gulf of Mexico. *Acta Botanica Mexicana* 107, 121–151.
- Pitts, P.A., 1993. Coastal upwelling of the central Florida Atlantic coast: cold near-shore waters during summer months surprise many divers. In: Heine, J.N., Crane, N.L. (Eds.), *Proceedings of the American Academy of Underwater Sciences Thirteenth Annual Scientific Diving Symposium*, Pacific Grove, CA, 19–22 September 1993. American Academy of Underwater Sciences, Dauphin Island, AL, pp. 99–106.
- Radke, E.G., Grattan, L.M., Cook, R.L., Smith, T.B., Anderson, D.M., Morris Jr., J.G., 2013. Ciguatera incidence in the U.S. Virgin Islands has not increased over a 30-year time period despite rising seawater temperatures. *Am. J. Trop. Med. Hyg.* 88, 908–913, <http://dx.doi.org/10.4269/ajtmh.12-0676>.
- Selig, E.R., Harvell, C.D., Bruno, J.F., Willis, B.L., Page, C.A., Casey, K.S., Sweatman, H., 2006. Analyzing the relationship between ocean temperature anomalies and coral disease outbreaks at broad spatial scales. In: Phinney, J.T., Hoegh-Guldberg, O., Kleypas, J., Skirving, W., Strong, A. (Eds.), *Coral Reefs and Climate Change: Science and Management*. American Geophysical Union, Washington, DC, pp. 111–128, <http://dx.doi.org/10.1029/61CE07>.
- Skinner, M.P., Brewer, T.D., Johnstone, R., Fleming, L.E., Lewis, R.J., 2011. Ciguatera fish poisoning in the Pacific Islands (1998 to 2008). *PLoS Negl. Trop. Dis.* 5, e1416, <http://dx.doi.org/10.1371/journal.pntd.0001416>.
- Smayda, T.J., 1997. Harmful algal blooms: their ecophysiology and general relevance to phytoplankton blooms in the sea. *Limnol. Oceanogr.* 42, 1137–1153, <http://dx.doi.org/10.4319/lo.1997.42.5.part.2.1137>.
- Smith, T.M., Reynolds, R.W., Peterson, T.C., Lawrimore, J., 2008. Improvements to NOAA's historical merged Land–Ocean Temperature analysis (1880–2006). *J. Climate* 21, 2283–2296, <http://dx.doi.org/10.1175/2007JCLI2100.1>.

- Strong, A.E., Liu, G., Eakin, C.M., Christensen, J.D., Skirving, W., Gledhill, D.K., Heron, S.F., Morgan, J.A., 2008. Implications for our coral reefs in a changing climate over the next few decades – hints from the past 22 years. In: Proceedings of the 11th International Coral Reef Symposium, vol. 2, Fort Lauderdale, Florida, 7–11 July 2008, pp. 1130–1334. Available from: <http://www.nova.edu/ncri/11icrs/> (accessed 20.05.15).
- Taylor, F.J.R., 1985. The distribution of the dinoflagellates *Gambierdiscus toxicus* in the eastern Caribbean. In: Gabrie, C., Salvat, B. (Eds.), Proceedings of the 5th International Coral Reef Congress, vol. 4. Antenne Museum, EPHE, Tahiti, pp. 423–428.
- Taylor, F.J.R., Gustavson, M.S., 1985. An underwater survey of the organism chiefly responsible for “ciguatera” fish poisoning in the eastern Caribbean region: the benthic dinoflagellate *Gambierdiscus toxicus*. In: Stefanon, A., Flemming, N.J. (Eds.), Proceedings of the Seventh International Diving Science Symposium. Padova University, Padova, Italy, pp. 95–111.
- Tester, P.A., Feldman, R.L., Nau, A.W., Kibler, S.R., Litaker, R.W., 2010. Ciguatera fish poisoning and sea surface temperatures in the Caribbean Sea and the West Indies. *Toxicon* 56, 698–710, <http://dx.doi.org/10.1016/j.toxicon.2010.02.026>.
- Tester, P.A., Kibler, S.R., Holland, W.C., Usup, G., Vandersea, M.W., Leaw, C.P., Teen, L.P., Larsen, J., Mohammad-Noor, N., Faust, M.A., Litaker, R.W., 2014. Sampling harmful benthic dinoflagellates: comparison of artificial and natural substrate methods. *Harmful Algae* 39, 8–25, <http://dx.doi.org/10.1016/j.hal.2014.06.009>.
- Tester, P.A., Vandersea, M.W., Buckel, C.A., Kibler, S.R., Holland, W.C., Davenport, E.D., Clark, R.D., Edwards, K.F., Taylor, J.C., Vander Pluym, J.L., Hickerson, E.L., Litaker, R.W., 2013. *Gambierdiscus* (Dinophyceae) species diversity in the Flower Garden Banks National Marine Sanctuary, Northern Gulf of Mexico, USA. *Harmful Algae* 29, 1–9, <http://dx.doi.org/10.1016/j.hal.2013.07.001>.
- Thiel, M., Gutow, L., 2005. The ecology of rafting in the marine environment. II. The rafting organisms and community. *Oceanogr. Mar. Biol. Ann. Rev.* 43, 279–418, <http://dx.doi.org/10.1201/9781420037449.ch7>.
- Tosteson, T.R., 2004. Caribbean ciguatera: a changing paradigm. *Rev. Biol. Trop.* 52, 109–113.
- Tosteson, T.R., Ballantine, D.L., Durst, H.D., 1988. Seasonal frequency of ciguatoxic barracuda in southwest Puerto Rico. *Toxicon* 26, 795–801, [http://dx.doi.org/10.1016/0041-0101\(88\)90320-0](http://dx.doi.org/10.1016/0041-0101(88)90320-0).
- Vandersea, M.W., Kibler, S.R., Holland, W.C., Tester, P.A., Schultz, T.F., Faust, M.A., Holmes, M.J., Chinain, M., Litaker, R.W., 2012. Development of semi-quantitative PCR assays for the detection and enumeration of *Gambierdiscus* species (Gonyaulacales, Dinophyceae). *J. Phycol.* 48, 902–915, <http://dx.doi.org/10.1111/j.1529-8817.2012.01146.x>.
- World Climate Research Programme (WCRP), 2015. WCRP Working Group on Coupled Modeling. WCRP (accessed 19.05.15) <http://www.wcrp-climate.org/wgcm/>.
- Zar, J.H., 1996. *Biostatistical Analysis*, third ed. Prentice Hall, Upper Saddle River, NJ.
- Zavala-Hidalgo, J., Gallegos-García, A., Martínez-Lopez, B., Morey, S.L., O'Brien, J.J., 2006. Seasonal upwelling on the western and southern shelves of the Gulf of Mexico. *Ocean Dyn.* 56, 333–338, <http://dx.doi.org/10.1007/s10236-006-0072-3>.